Effects of different configurations of inclined double-cutoff walls beneath hydraulic structures on uplift forces, seepage discharge and exit hydraulic gradient

Asaad M. Armanuos, Abdelazim M. Negm, Akbar A. Javadi, and Tamer A. Gado

[1]Irrigation and Hydraulics Engineering Department, Civil Engineering Department, Faculty of Engineering, Tanta University, 31512 Tanta, Egypt; Email: asaad.matter@f-eng.tanta.edu.eg

[2]Water and Water Structures Engineering Department, Faculty of Engineering, Zagazig University, Zagazig 44519, Egypt, Email: amnegm85@yahoo.com, amnegm@zu.edu.eg

[3]Computational Geomechanics Group, Department of Engineering, University of Exeter, North Park Road, Exeter EX4 4QF, UK, Email: a.a.javadi@ex.ac.uk

[4]Department of Irrigation and Hydraulics Engineering, Faculty of Engineering, Tanta University, Tanta, Egypt, Email: tamer.gado@f-eng.tanta.edu.eg

Abstract

In design of hydraulic structures, using cutoff walls is essential to reduce and control the resultant uplift force (*U*), seepage discharge (*Q*), and exit hydraulic gradient (*i*). Typically, double cutoff walls in the upstream and downstream ends are required to decrease the uplift force and to minimize the exit hydraulic gradient, respectively. This study aims to investigate the effectiveness of inclined double cutoff walls under hydraulic structures, considering the influence of depths, locations, and inclination angles of the upstream and downstream cutoff walls. Finite Element Method (FEM) was used to solve the groundwater flow equations with specified boundary conditions. The relative error between the numerical and analytical solutions for the case of equal depths of cutoff walls confirmed that FEM can be used to predict the values of *U*, *i*, and *Q* with maximum of 5% error. The results also confirmed that using deeper cutoff wall on the upstream side than the downstream wall can result in a reduction of the uplift force. In addition, positioning the downstream cutoff wall closer to the upstream wall leads to further reduction of the uplift force compared to the cutoff walls fixed at the upstream and downstream ends. Installing a deeper cutoff wall on the downstream side results in more reduction in the exit hydraulic gradient. In the case of the cutoff walls located in the upstream and downstream ends, the exit hydraulic gradient will be less than when the cutoff walls are installed at a closer distance. Increasing the inclination angle of the downstream cutoff wall has a significant effect on reduction of the exit hydraulic gradient. Embedment of the cutoff walls in the upstream and downstream ends with right angles and equal depths reduces the seepage discharge more than other cases. The results of this study can help designers of hydraulic structures to efficiently align the cutoff walls to control uplift force, exit gradient, and seepage discharge.

Keywords: Inclined cutoff walls, Hydraulic structures, Uplift force, Exit hydraulic gradient, Seepage discharge

Introduction:

Seepage occurs under the base of some hydraulic structures (e.g., gravity dams, weirs, diversion dams, or stilling basins built on permeable foundation), due to the hydraulic head difference between upstream and downstream sides of these structures. The effects of seepage on the base of hydraulic structures can include uplift force, exit hydraulic gradient, and seepage discharge. Uplift force diminishes the shear resistance

between the structure and its base and reduces the resistance of the structure against sliding or overtopping. Increasing seepage velocity under hydraulic structures can accelerate the piping phenomenon, causing soil erosion at the exit point/region of hydraulic structures. In addition, high values of exit hydraulic gradient can cause the movement of particles of foundation soil, potentially leading to instability problem. Subsequently, design of hydraulic structures should limit the uplift force, seepage discharge, and exit hydraulic gradient.

Bligh (1910) presented the first empirical method to control the exit hydraulic gradient and uplift force, and the creep length theory for the seepage discharge under hydraulic structures. Based on the investigation of more than 200 damaged hydraulic structures, Lane (1935) reported that there is a significant difference between the horizontal and vertical creep paths, and introduced the weighted creep theory for seepage flow under hydraulic structures, giving weighted coefficients for the total percolation lengths in horizontal and vertical directions. Khosla et al. (1936) introduced a theoretical method, based on complex numbers, to determine the exit gradient and uplift force for foundation of hydraulic structures. Considering the complexity of the proposed solution, they presented simple charts to facilitate the design process. Malhotra (1936) proposed a method for analysis of seepage with double cutoff walls with equal depth in the upstream and downstream of an apron. The method assumed that the apron foundation is of infinite depth, which is unrealistic. In many cases, hydraulic structures may have cutoff walls with unequal depths. Pavlovsky (1956 and 1962) presented analytical solutions for two instances of finite seepage depth: flat foundation with a single cutoff wall, and depressed floors without cutoff walls. His work, which was originally written in Russian, was later translated to English (Harr 1962; Polubarinova-Kochina 1962).

Chawla and Kumar (1983) introduced an analytical solution for flat foundations incorporating two cutoff walls with a finite permeable foundation. Najjar and Naouss (1999) examined seepage discharge rates and exit gradients under a cutoff wall in a non-homogeneous soil using the finite element method (FEM). Goel and Pillai (2010) presented a method to control the exit hydraulic gradient with implemented stone protection (rip-rap) and an end cutoff wall in aprons with unlimited depth of permeable foundation. Jain and Reddi (2011) proposed a closed form solution for estimation of the uplift force and exit hydraulic gradient at key points under the apron. The constraint in their investigation was the supposition of equivalent depth of cutoff walls at the apron ends. Salmasi et al. (2015) utilized alleviation wells downstream of embankment dams to diminish uplift force. These wells collect the leaked water beneath the dam foundation and in this way, they prevent the development of excessive pore water pressure and the piping phenomenon at the toe of the dam.

Some researchers have utilized upstream semi-impermeable blankets to decrease the uplift force and seepage flow (Salmasi and Nouri, 2017). These blankets, which are normally constructed by compaction of clay, extend the creep length. This results in more energy loss, compared with the case without blankets, at the upstream of the hydraulic structure. Nourani et al. (2017) investigated the optimum position for vertical drains located in gravity dams. They utilized the FEM to predict the uplift force with and without vertical drains in the dam foundation. In design of dams, it is important to minimize the total resultant uplift force. The minimized uplift forces make the dam more stable against the existing loads and helps to achieve an economical design. It was shown that vertical drains in the dam foundation can collect most of the infiltered water.

Koupaei (1991) argued that the amount of uplift pressure predicted by Bligh (1910) and Lane (1935) methods is less than Khosla et al. 1936 and the Finite Difference Methods (FDM). By combining the concept of random fields and the Finite Element Method, Griffiths and Fenton (1997) presented a 3D steady

state seepage model in which the permeability was randomly distributed through the soil body. Opyrchał (2003) introduced the use of the fuzzy concept to distinguish the creep path within the body of a dam. Sedghi asl et al. (2005) utilized the FDM to examine the effect of the position of a cutoff wall in reducing the seepage discharge and velocity beneath hydraulic structures and found that the best position for the cutoff wall is at the upstream and downstream ends. Rahmani and Afshar (2007) introduced a meshless strategy, using the discrete least square technique (DLSM), for analysis of free surface seepage flow. The results showed a good estimation in case of regular and irregular nodes positioning. Ahmed and Bazaraa (2009) studied 3D seepage discharge beneath and around hydraulic structures using a finite element model. They compared 3D and 2D analyses for estimating the exit hydraulic gradient, uplift force, and seepage flow.

Focusing on diminishing seepage losses through irrigation canal banks and stable hydraulic structures, Ahmed (2011) studied the impacts of various arrangements of a sheet pile wall on the decrease of uplift force, exit hydraulic gradient, and seepage flow. He proposed a clay core at the inward edge of the banks. Based on the results of an experimental research, Sedghi asl et al. (2011) proposed a number of rules to determine the optimum length of clay blanket and the depth of cutoff walls to minimize uplift pressure against protective dikes.

Zainal (2011) studied the effects of cutoff wall inclination on seepage beneath dams and showed that the best angles to limit the seepage flow, exit hydraulic gradient, and uplift force are about 60°, 120° to 135°, and 45° to 75°, respectively. Jafarieh and Ghannad (2014) investigated the effect of foundation uplift force on elastic reaction of soil-structure system and indicated that a large foundation uplift force can decrease the drift reaction of structures.

The present study investigates the effect of inclined double cutoff walls on uplift force, exit hydraulic gradient, and seepage rate. Different configurations of depths, locations, and inclination angles of the upstream and downstream cutoff walls are considered. The governing groundwater flow equations are solved using FEM through Geo-Studio software. Validation of the results is performed by comparison with the closed-form solution presented by Jain and Reddi (2011).

Material and methods

Governing equations of the numerical model

The following equation presents the flow through a porous medium. It is a combination of continuity equation and Darcy's law (or Richards equation) (Geo-Studio, 2012).

$$\frac{\partial}{\partial t}(\rho\theta) = \left[\frac{\partial}{\partial x}\left(\rho k_x \frac{\partial h}{\partial x}\right) + \frac{\partial}{\partial y}\left(\rho k_y \frac{\partial h}{\partial y}\right) + \frac{\partial}{\partial z}\left(\rho k_z \frac{\partial h}{\partial z}\right)\right] \quad (1)$$

where h is the total hydraulic head [L], k_x, k_y, and k_z are the hydraulic conductivity of the porous medium in x-, y-, and z-directions, respectively [L/T], ρ is the density of water [M/L^3], θ is the volumetric water content [L^3/L^3], and t is the time [T]. This equation expresses that the difference between the entering and leaving flow of an elemental volume is equal to the change in storage of the soil system. In the case of homogenous, anisotropic, unsaturated, and incompressible porous medium, equation 1 can be written as follows:

$$\frac{\partial}{\partial x}\left(k_x \frac{\partial h}{\partial x}\right) + \frac{\partial}{\partial y}\left(k_y \frac{\partial h}{\partial y}\right) + \frac{\partial}{\partial z}\left(k_z \frac{\partial h}{\partial z}\right) = \frac{\partial \theta}{\partial t} \quad (2)$$

In the case of a homogenous, isotropic (k_x=k_y=k_z= constant= k), and saturated porous medium ($\frac{\partial \theta}{\partial t} = 0$), equation 2 becomes Laplace equation (Richards equation):

$$\frac{\partial^2 h}{\partial x^2} + \frac{\partial^2 h}{\partial y^2} + \frac{\partial^2 h}{\partial z^2} = 0 \quad (3)$$

A flow net can be used as the graphical solution for the Laplace equation. A flow net is a contours map consisting of equipotential lines intersecting flow lines. For the flow net to be an accurate solution for the Laplace equation, the equipotential and flow lines must stick to specific rules, e.g., the equipotential lines should cross the flow lines with right angles. The zone between two contiguous flow lines is known as a flow channel and the seepage flow through any flow channel is equivalent to the flow through any other flow channel. In the current study, the foundation of hydraulic structure is considered homogeneous and isotropic and the porous medium is assumed to be saturated.

The foundation of the structure is viewed as a single permeable medium with a saturated conductivity of k = 10^{-5} m/s. As the foundation of the structure is considered saturated, the saturated hydraulic conductivity is utilized in the numerical arrangement. The current research is completed utilizing the Geo-Studio software package. The SEEP/W solves the governing equation in the porous medium (Laplace equation) with specified boundary conditions utilizing the finite element method (FEM).

Numerical simulation using finite element method (FEM)

Fig. 1 presents various arrangements of inclined double cutoff walls under a hydraulic structure. In Fig. 1 (upper left), two key points *C* and *E* are used to estimate the uplift pressure. Point *C* is located (left) of the downstream cutoff wall and key point *E* is located to the right side of the upstream cutoff wall. The line from *C* to *E* represents the bottom of the structure (apron).

In view of the hydraulic parameters listed in Tables 1 and 2, a total of 631 numerical simulation runs are executed for the investigation. From these models, 630 numerical models involve the hydraulic structure with upstream and downstream cutoff walls and one numerical model is used for analysis of seepage without the two cutoff walls. Table 2 presents the dimensionless values of the studied parameters. The 630 numerical models are divided into two groups: 315 runs for the case of L/B=0.5, where the downstream cutoff wall was embedded close to the upstream wall and the other 315 runs for the case of L/B=1.0, where the downstream cutoff wall was fixed at the right end boundary of the hydraulic structure. In addition, the 630 numerical runs can be divided into 3 groups of 210 runs for the following cases: d_2/d_1=0.5, d_2=d_1, and d_2/d_1=2.0.

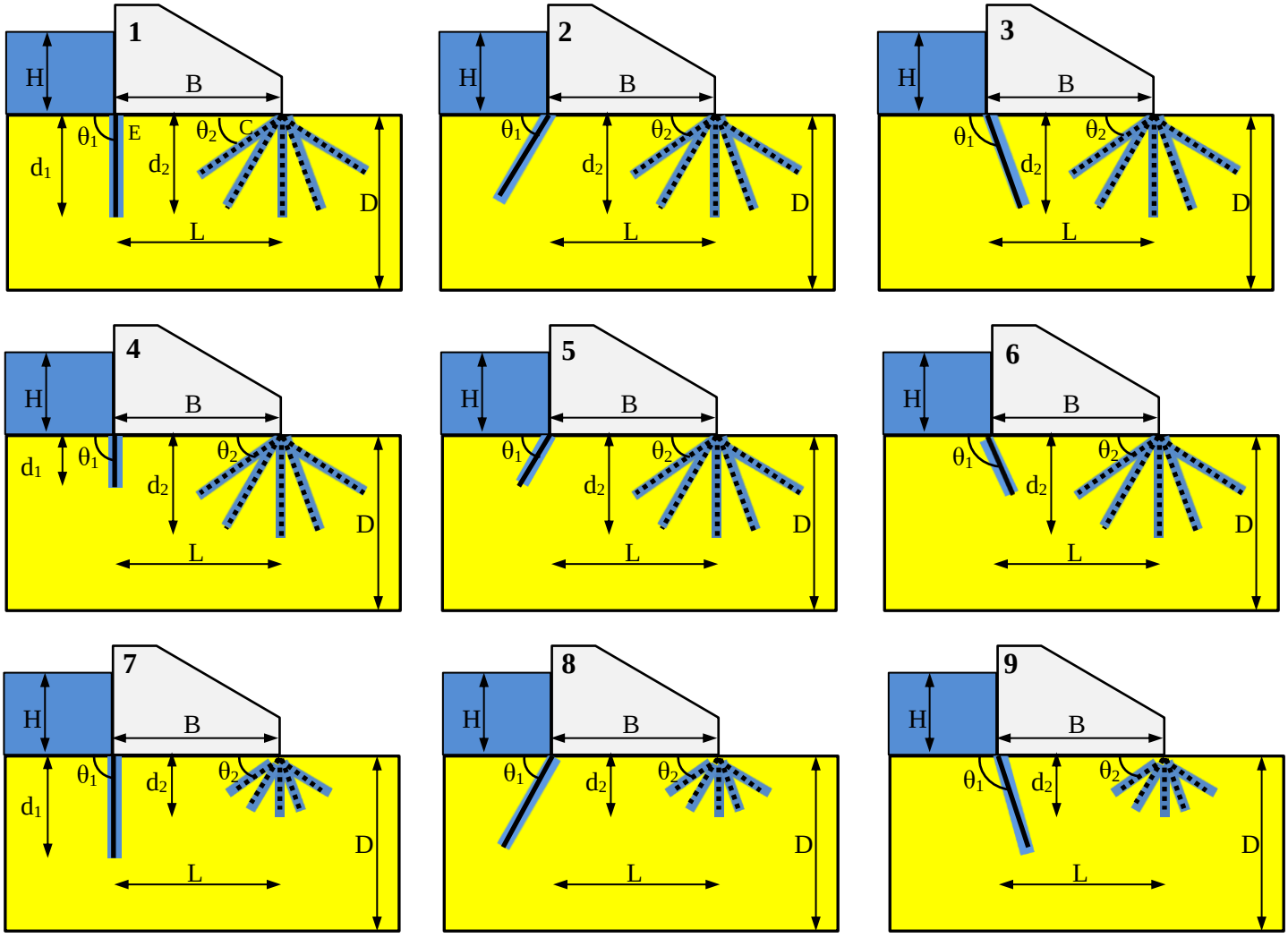
1
H
B
θ1
E
θ2
C
d1
d2
D
L
2
H
B
θ1
θ2
d2
D
L
3
H
B
θ1
θ2
d2
D
L
4
H
B
θ1
θ2
d1
d2
D
L
5
H
B
θ1
θ2
d2
D
L
6
H
B
θ1
θ2
d2
D
L
7
H
B
θ1
d2
θ2
d1
D
L
8
H
B
θ1
d2
θ2
D
L
9
H
B
θ1
d2
θ2
D
L

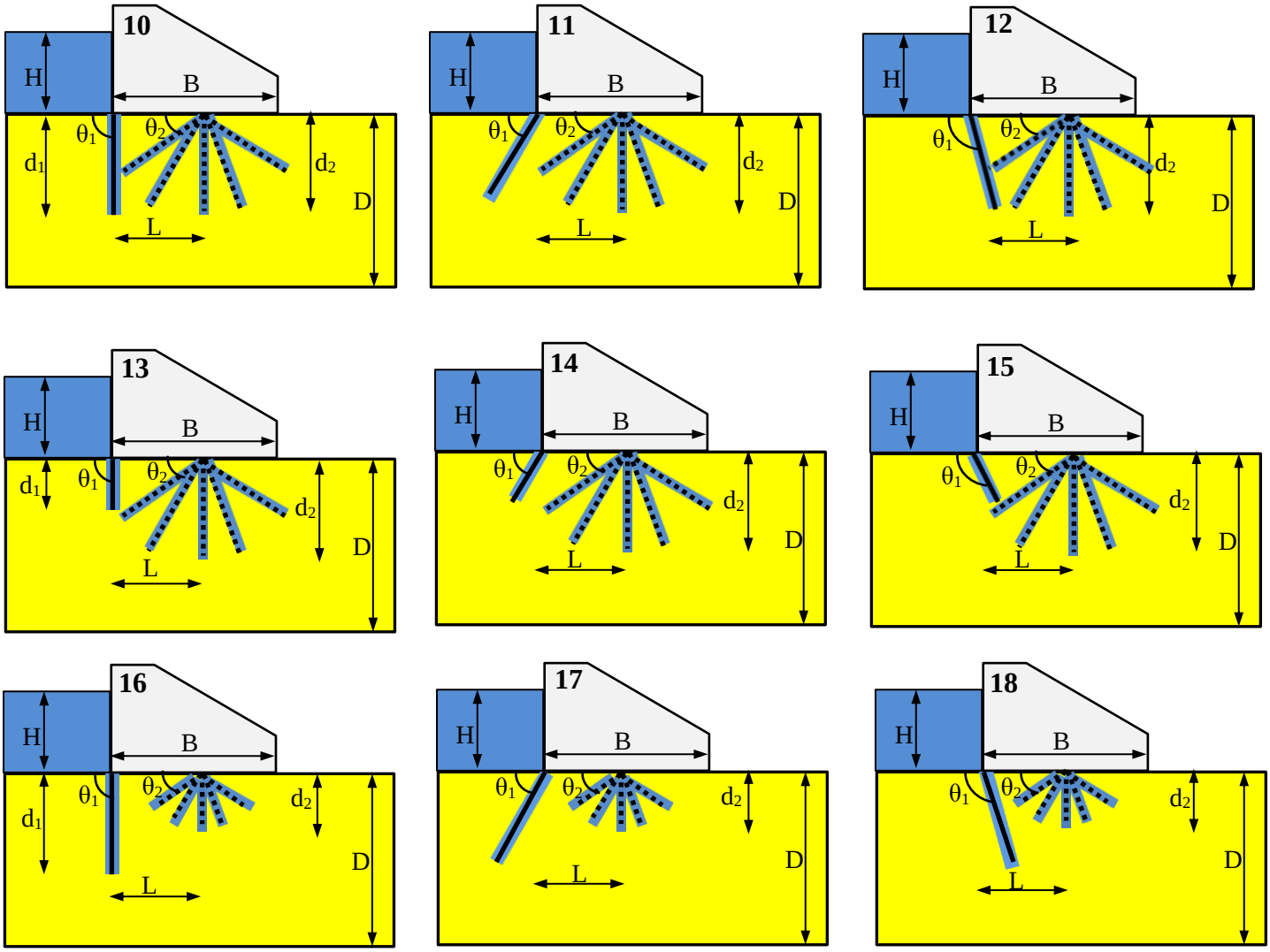

d_1 is the depth of upstream cutoff wall, θ_1 is the inclination angle of the upstream cutoff wall, d_2 is the depth of downstream cutoff wall, θ_2 is the inclination angle of the downstream cutoff wall, L is the distance between the upstream and downstream cutoff walls, D is the depth of the pervious foundation, B is the width of the hydraulic structure, and H is the upstream water head of the hydraulic structure.

Fig. 1. Different configurations of inclined double cutoff walls beneath the hydraulic structure

Table 1: Definition of parameters

Parameter	Definition
d_1	The depth of upstream cutoff wall [m]
d_2	The depth of downstream cutoff wall [m]
B	The width of hydraulic structure (apron) [m]
D	The depth of permeable layer [m]
i	Hydraulic gradient with using cutoff walls [m]
i_o	Hydraulic gradient without using cutoff walls [m]
i/i_o	Relative exit hydraulic gradient
H	Upstream pressure head of the hydraulic structure [m]
L	The distance from the upstream cutoff wall to the downstream cutoff wall [m]
Q	The seepage discharge under the hydraulic structure with cutoff walls [m^3/sec]
Q_o	The seepage discharge under the hydraulic structure without cutoff walls [m^3/sec]
Q/Q_o	Relative seepage discharge
h	Total head of the hydraulic structure [m]
t	Time [Sec]
U	The uplift force under the hydraulic structure with cutoff walls
U_o	The uplift force under the hydraulic structure without cutoff walls
U/U_o	Relative uplift force
g	Gravity acceleration [m/sec^2]
ρ	The density of the water [kg/m^3]
k_x	The hydraulic conductivity of the porous medium in x-direction [m/sec]
k_y	The hydraulic conductivity of the porous medium in y-direction [m/sec]
k_z	The hydraulic conductivity of the porous medium in z-direction [m/sec]
θ_1	The inclination angle of upstream cutoff wall
θ_2	The inclination angle of downstream cutoff wall
b	The left end boundary in the upstream or the right end boundary in the downstream

Table 2: Dimensionless values of the studied parameters

Dimensionless Parameter	Values						
L/B	0.5	1.0					
d_2/D	0.2	0.3	0.4	0.5	0.6	0.7	0.8
θ_1	60	90	120				
θ_2	30	60	90	120	150		
d_2/d_1	0.5	1.0	2.0				

Fig. 2 shows the details of the boundary conditions for the numerical simulation. At the upstream end, the boundary condition is characterized as the pressure head which is assigned by *H*. The pressure head at the

downstream end is equal to zero. In Fig. 2, the inclination angle of the upstream cutoff wall (θ_1) is 60°, and the inclination angle of the downstream cutoff wall (θ_2) is 120°. The boundary conditions used are: upstream total head (h)=40m or (the upstream pressure head (H)=25m), downstream total head (h)=15m, or (the downstream pressure head (H)=0.0 m), the horizontal and vertical boundaries of foundation are impermeable, and the boundary in the base of structure's foundation is impermeable.

The two-dimensional domain considered in the model is 90 m (length) by 15 m (depth). The total number of elements in the domain (NE) = 15000, giving the number of elements per the unit area of the domain (NE/A) = 11). The saturated hydraulic conductivity of the soil K = $1x10^{-5}$ m/sec.

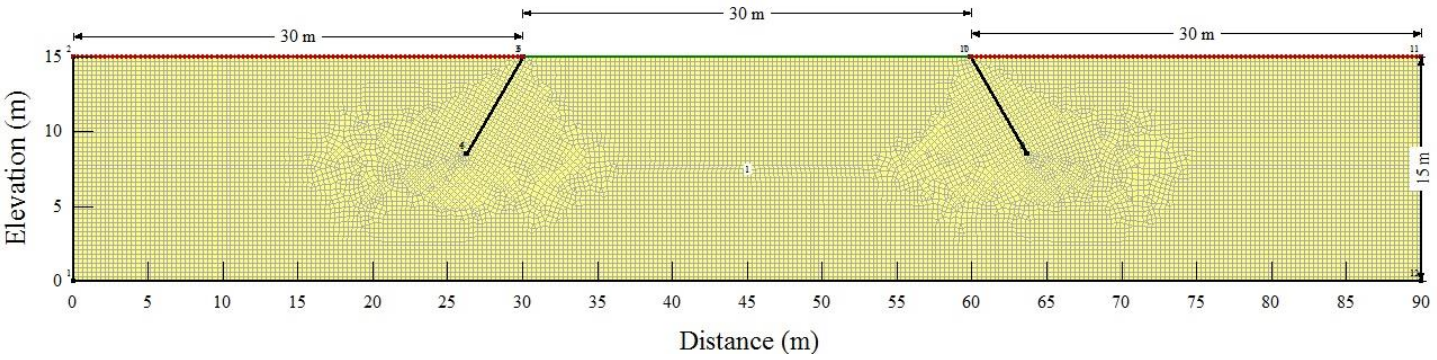

Fig. 2. The boundary conditions used for the numerical simulation for the case: L/B = 1, d_2/d_1 = 1.0, d_1=0.5D, θ_1 = 60°, and θ_2 = 120°.

The base of the domain, the base of the hydraulic structure and the upstream and downstream cutoff walls are characterized as impermeable boundary conditions. The soil is considered saturated and isotropic (k_x=k_y). The domain is discretized with quadrilateral and triangular elements to improve accuracy. Before starting the numerical simulations, a mesh-independence test is carried out to determine the optimal number of elements essential for accurate finite element model calculations. For this, the percent of relative blunder (R_E%) is acquired for the numerical simulations utilizing various numbers of mesh elements. The calculation of R_E% depends on the values of the hydraulic gradient and pressure head at the key point C. That is, the difference between the hydraulic gradient from numerical simulation is compared with the computed value from the analytical solution of Jain and Reddi (2011) and is characterized as an error for hydraulic gradient, and this relative error is calculated for different meshes, as shown in Fig 3a. In addition, the difference between the pressure head from numerical simulation at the key point C is compared with the computed value from the analytical solution of Jain and Reddi (2011) and is characterized as the relative error for pressure head, as shown in Fig 3b. The outcomes show (Fig. 3) that by increasing the number of elements up to 15000, the percent value of relative error (R_E%) turns out to be less than 0.2% for Fig. 3.a, and 1% for Fig. 3.b.

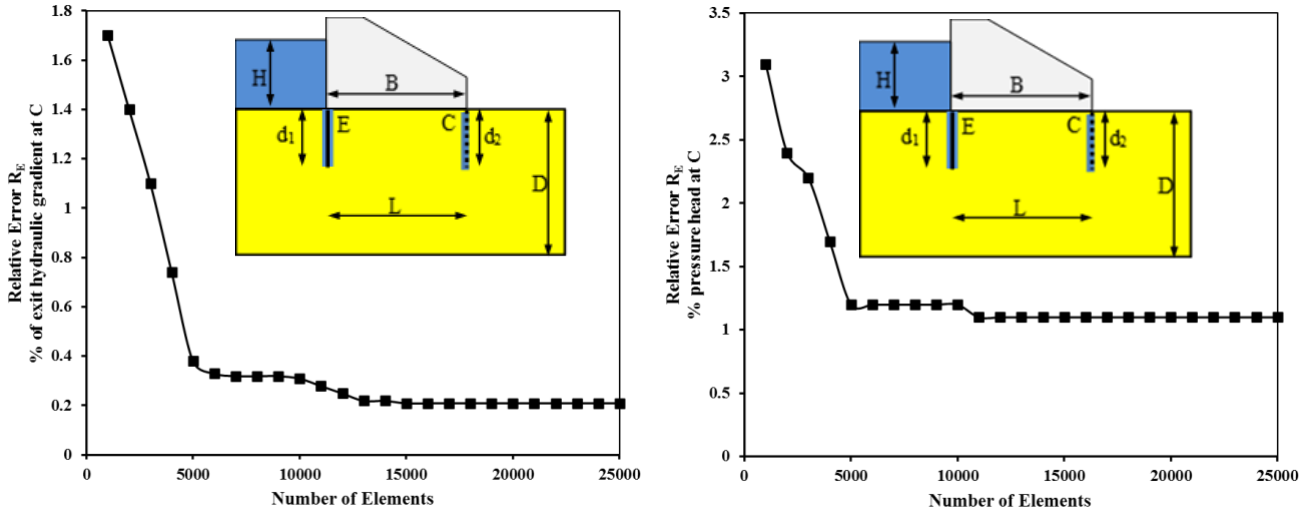

(a) (b)

Fig. 3. The relative error (R_E %) values corresponding to different number of used elements for: (a) the relative hydraulic gradient at key point *C*, and (b) the pressure head at key point C

It is noticed that the RE% is practically constant when the number of elements is more than 15,000. Therefore, this number of elements is chosen for further numerical runs in the following analyses. Fig. 2 presents the boundary conditions for the numerical runs with L/B = 1, d_2/d_1 = 1.0, d_2=0.5D. In this case, the dimension of the quadrilateral and triangular elements is equal to 0.3 m and the number of nodes and elements are equal to 15,391 and 15077, respectively (Fig. 2). The upstream cutoff wall is located at x = 30 m with inclination angle θ_1 = 60^o and the downstream cutoff wall is located at x = 60 m with inclination angle θ_2 = 120^o.

The steps of numerical simulations in the FEM are introduced in Fig. 4. This procedure includes the following steps: building of geometric numerical model, the generations of mesh, description of material properties, design of boundary conditions, the governing equation solutions alongside the boundary conditions, and visualizing and understanding of the outcomes. If there is a reasonable understanding between the results of numerical simulation with the analytical solution, the procedure of numerical modeling is agreed. During the procedure of numerical modeling, a modeler can refine the outputs of numerical simulation results by playing out the accompanying steps, as shown in Fig. 4: increasing the number of elements through utilizing a finer mesh, changing the hydraulic conductivity of the soil, and modifying the model bindery conditions.

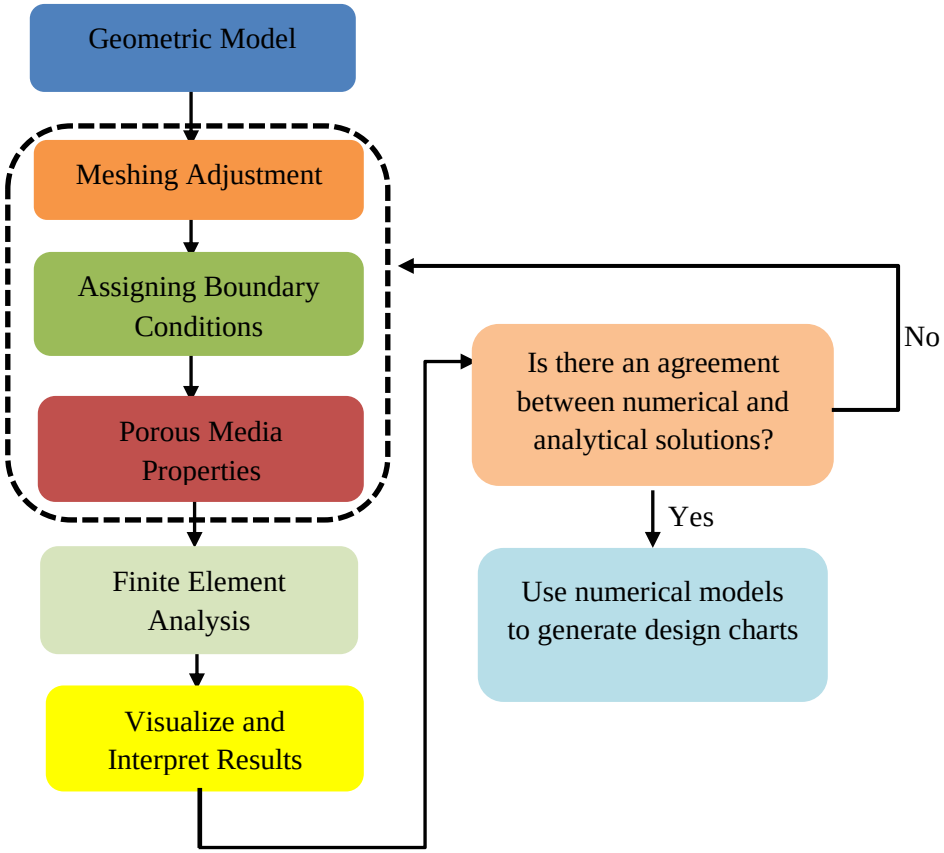

Fig. 4. Simulation procedure for numerical Analysis

Determination of the minimum distance between the two end boundaries for independent checking of solutions

In this study, the total domain length in horizontal direction ($B+2b$) is 90 m with a vertical height of 15 m (D = 15 m), where B is the length of the apron =30m, and b is the distance from the left (upstream) cutoff wall to the left end boundary or from the right (downstream) cutoff wall to the right end boundary of the domain. In addition, the minimum distance of the upstream and the downstream end boundaries of the domain (b) is examined. In other words, by increasing the distance of the upstream and downstream end boundaries (b), it was shown that the position of these boundaries did not impact the results. In all numerical simulations, the number of elements per unit area of the study domain is fixed to 11 (NE/A = 11). Figs. 5 and 6 show the minimum distance required for the upstream and downstream end boundaries of the study domain. Fig. 5 presents the extension of upstream and downstream end boundaries and its effects on the numerical results, where the value of b/B was changed from 0.2 to 2.0. Fig. 6 shows the impact of upstream and downstream end boundaries on the relative error between the numerical and analytical solutions for the exit hydraulic gradient, hydraulic head at key point C, and seepage discharge (Q).

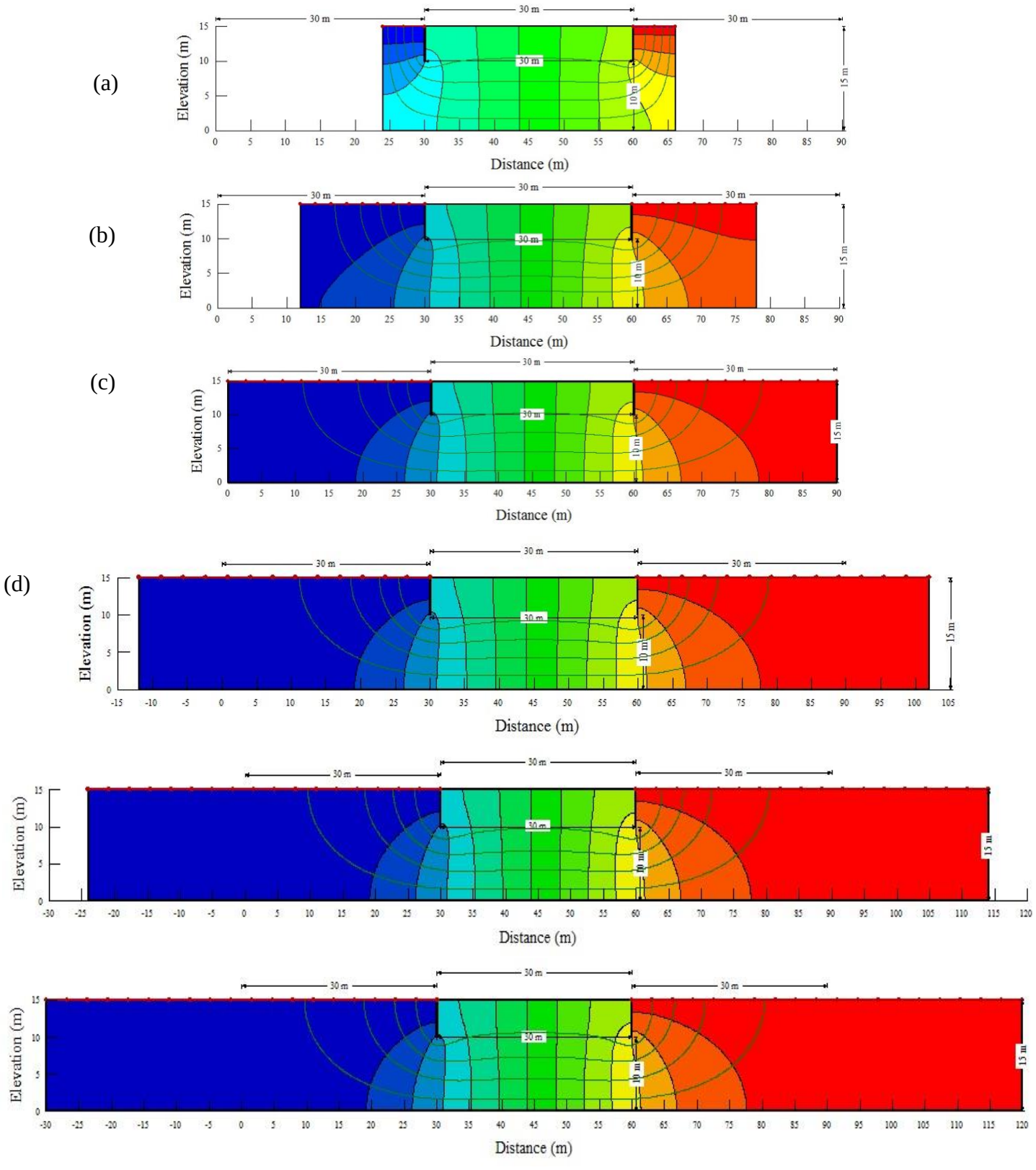

Fig. 5. The extension of the upstream and downstream end boundaries and their effects on numerical results in cases of: (a) *b/B*=0.2, (b) 0.60, (c) 1.0, (d) 1.4, (e) 1.8, and (f) 2.0

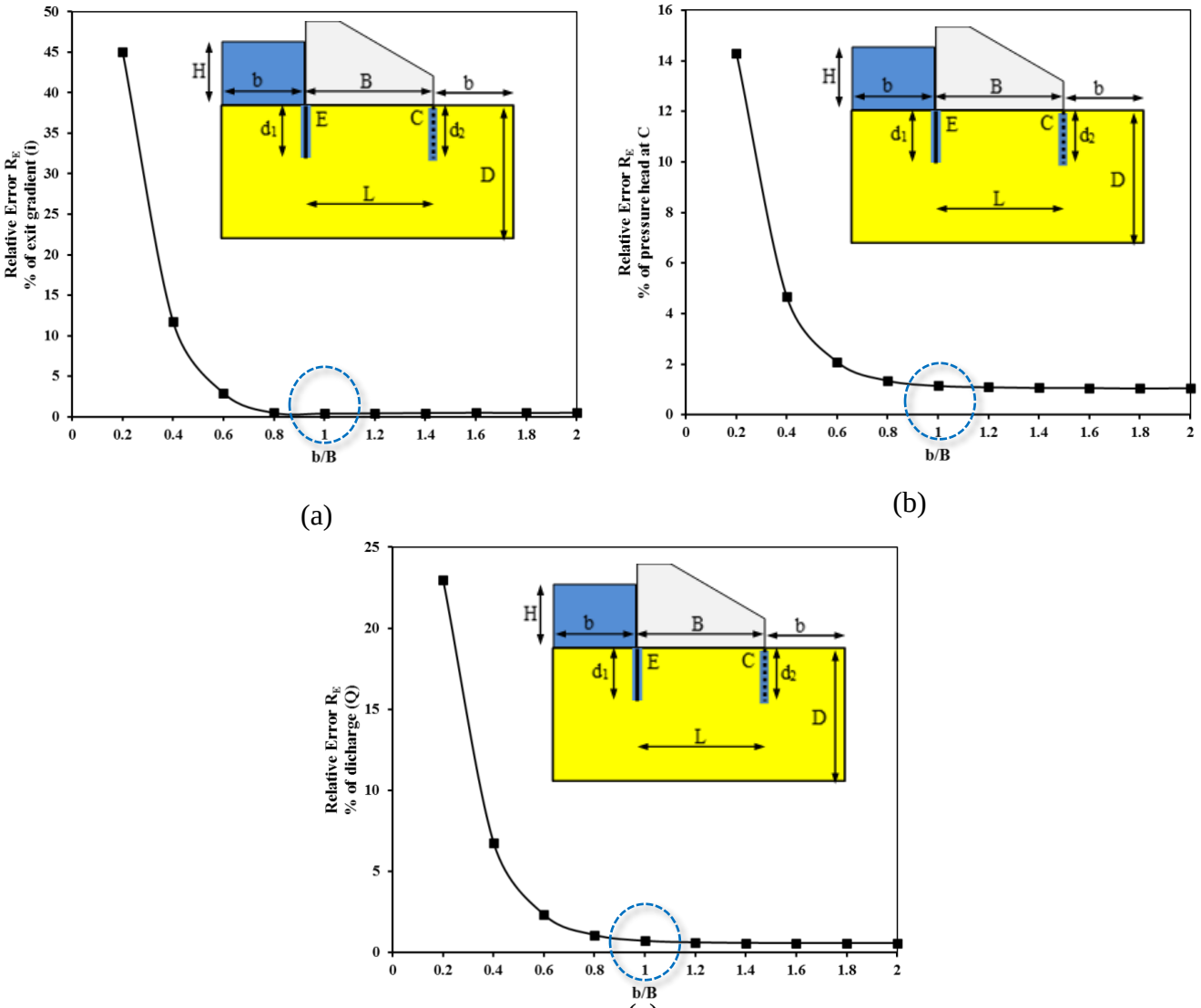

Fig. 6. The relation between relative error (R_E) % and the ratio of the end boundary (b/B) to determine the minimum distance between the upstream and downstream end boundaries for: (a) relative hydraulic gradient at key point *C*, (b) hydraulic head at key point *C*, (c) seepage discharge (Q)

Results and Discussion

Fig. 7 presents the flow net beneath the hydraulic structure in cases of with and without cutoff walls. The presented flow nets involve the flow lines and the equipotential lines obtained from the numerical simulations. In Fig. (7a), flow paths take the shape of ellipse while the equipotential curves take the shape of hyperbola. The values of the seepage discharge rate under the concrete apron are shown at the base of the hydraulic structure for all presented cases. For the example presented in Fig. (7a), the seepage discharge rate is 8.69 x 10^{-5} m^3/s per unit width of the hydraulic structure without using cutoff walls. Fig. 7b presents the flow net beneath the hydraulic structure using double cutoff walls with d_2/d_1 = 1.0, inclination angle θ_1 = 90°, and the downstream cutoff wall is located at x = 60 m with inclination angle θ_2 = 90°. The flow lines are concentrated more upstream and downstream of the hydraulic structure compared to the case without using cutoff walls (Fig. 7a); and thus, this case results in a greater loss in energy. The equipotential curves are more concentrated close to the cutoff walls than those on the case without using cutoff walls.

To validate the model, the results of the numerical simulation are compared with those of the analytical solutions of Jain and Reddi (2011), as shown in Fig. 8 which confirms an acceptable agreement (the maximum difference is less than 5%).

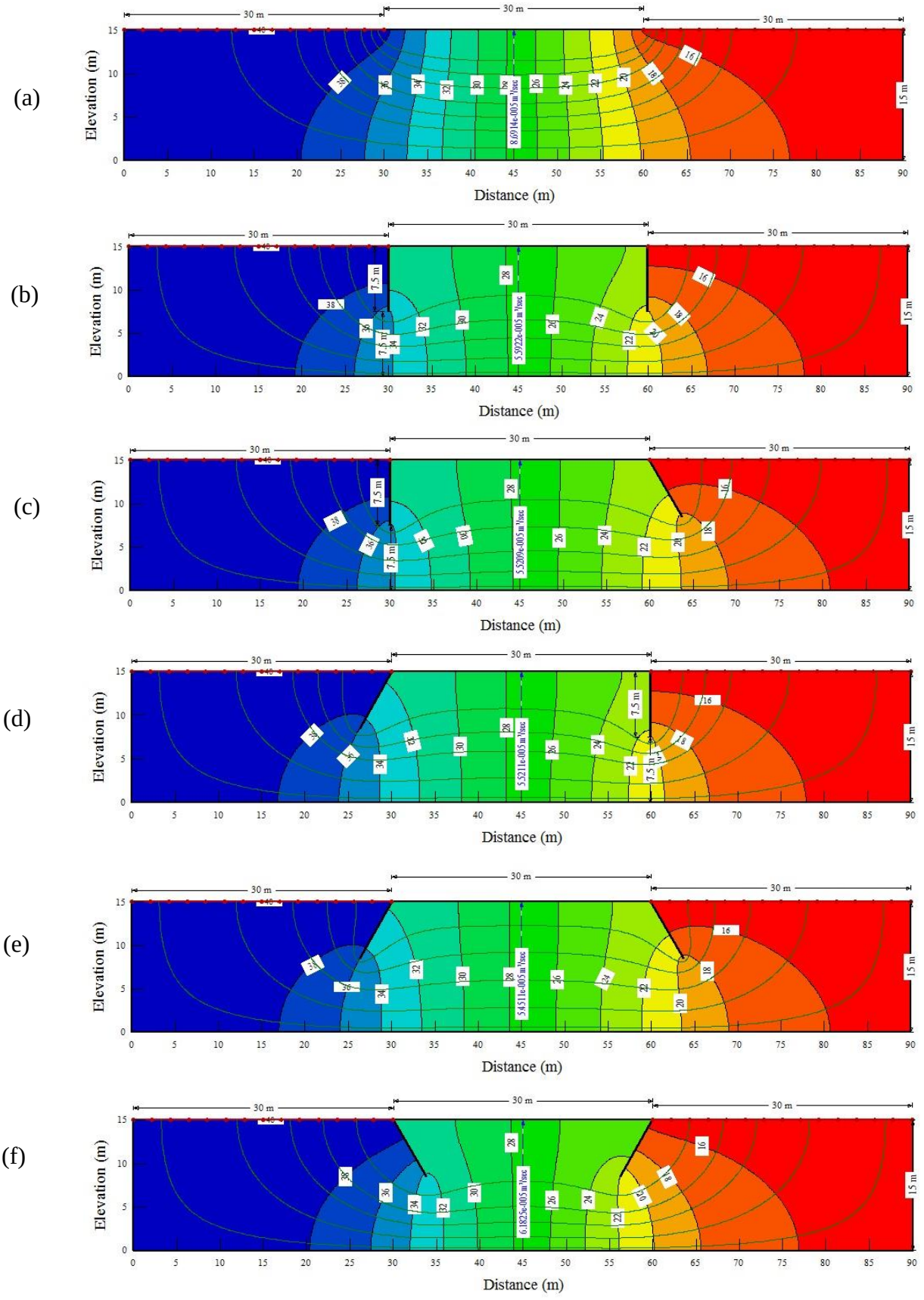

Fig. 7. The flow nets beneath the hydraulic structure in cases of: (a) without using cutoff walls, (b) $d_1=d_2$, $\theta_1 = \theta_2= 90^o$, (c) $d_1=d_2$, $\theta_1 =90^o$, $\theta_2= 120^o$, (d) $d_1=d_2$, $\theta_1 =60^o$, $\theta_2 = 90^o$, (e) $d_1=d_2$, $\theta_1 =60^o$, $\theta_2= 120^o$, (f) $d_1=d_2$, $\theta_1 =120^o$, $\theta_2 = 60^o$

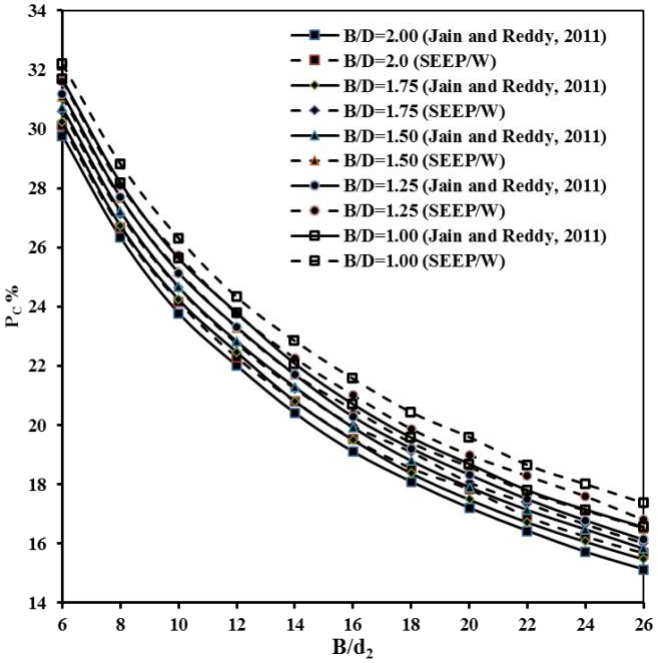

(a)

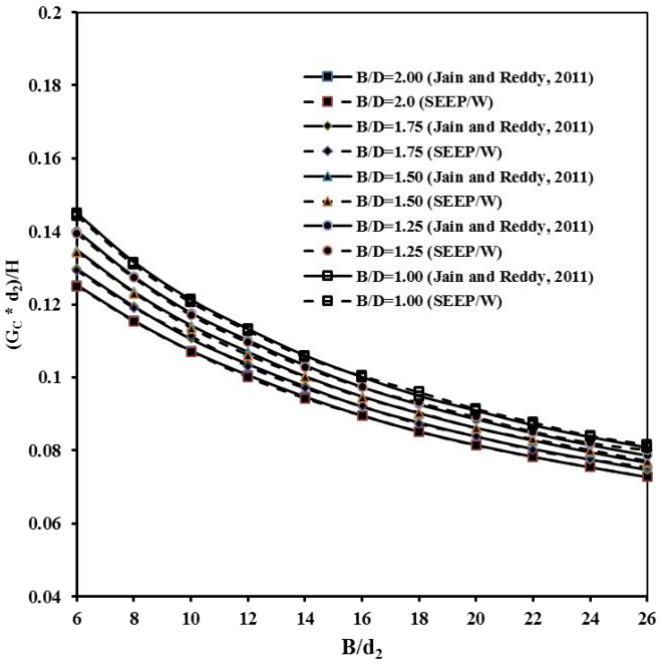

(b)

P_c is the percentage of the relative head characterized as $P_c = P/H \times 100$ (%), P is the pressure head at the key point C, i_c is the relative hydraulic gradient at point C, k is the hydraulic conductivity of the soil beneath the foundation of the dam (m/s), G_c is the hydraulic gradient at point C, q is the seepage discharge rate per unit width of the hydraulic structure (m^2/s), D is the depth of the pervious foundation, B is the width of the hydraulic structure, and H is the upstream water head of the hydraulic structure.

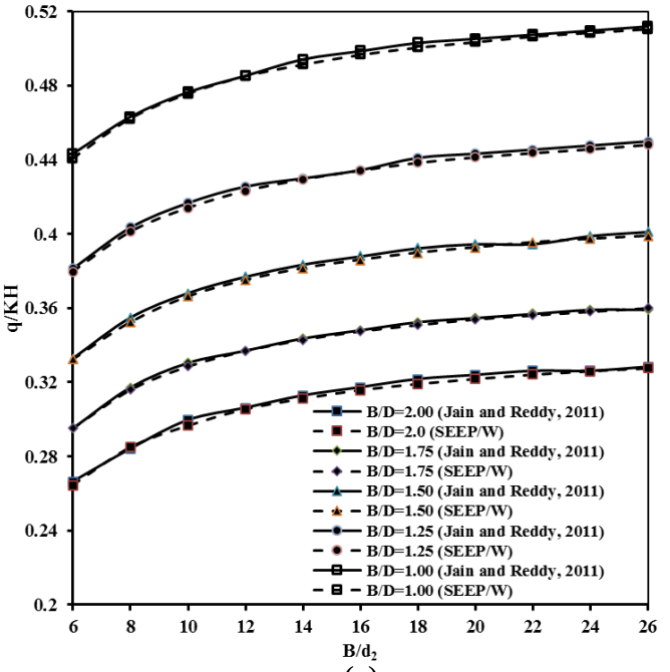

(c)

Fig. 8. Comparison between the results of the numerical model and the analytical results of Jain and Reddi (2011) study (for cutoff walls of equal depth, d_1=d_2, and L/B = 1) for: (a) relative uplift pressure at point *C*, (b) relative hydraulic gradient at point *C*, and (c) relative seepage discharge.

Effectiveness of inclined double cutoff walls in controlling uplift force:

Fig. 9 presents the variations of the relative uplift force (U/U_o) with the inclination angle of the downstream cutoff wall (θ_2) for $\theta_1 = 60^o$, $L/B = 0.5$, and for three cutoff wall depth ratios $d_2/d_1 = 0.5$, 1.0, and 2.0. U_o is the value of the uplift force without using cutoff walls and U is the uplift force value using two cutoff walls in the upstream and downstream. The results (Fig. 9) show that as the depth of the upstream and downstream cutoff walls (d_1 and d_2) increases, the values of uplift force decrease. For $d_2/d_1 = 0.5$ and d_2/d_1=1.0 as the inclination angle of the downstream cutoff wall (θ_2) increases, the resulting uplift force is relatively constant. As θ_2 increases beyond 90°, the uplift force decreases (Fig. 9(b)). For d_2/d_1=2.0, increasing the depth of the downstream cutoff wall (d_2) is less significant in reducing the uplift force compared with d_2/d_1=0.5 and 1.0 (Fig. 9(c)).

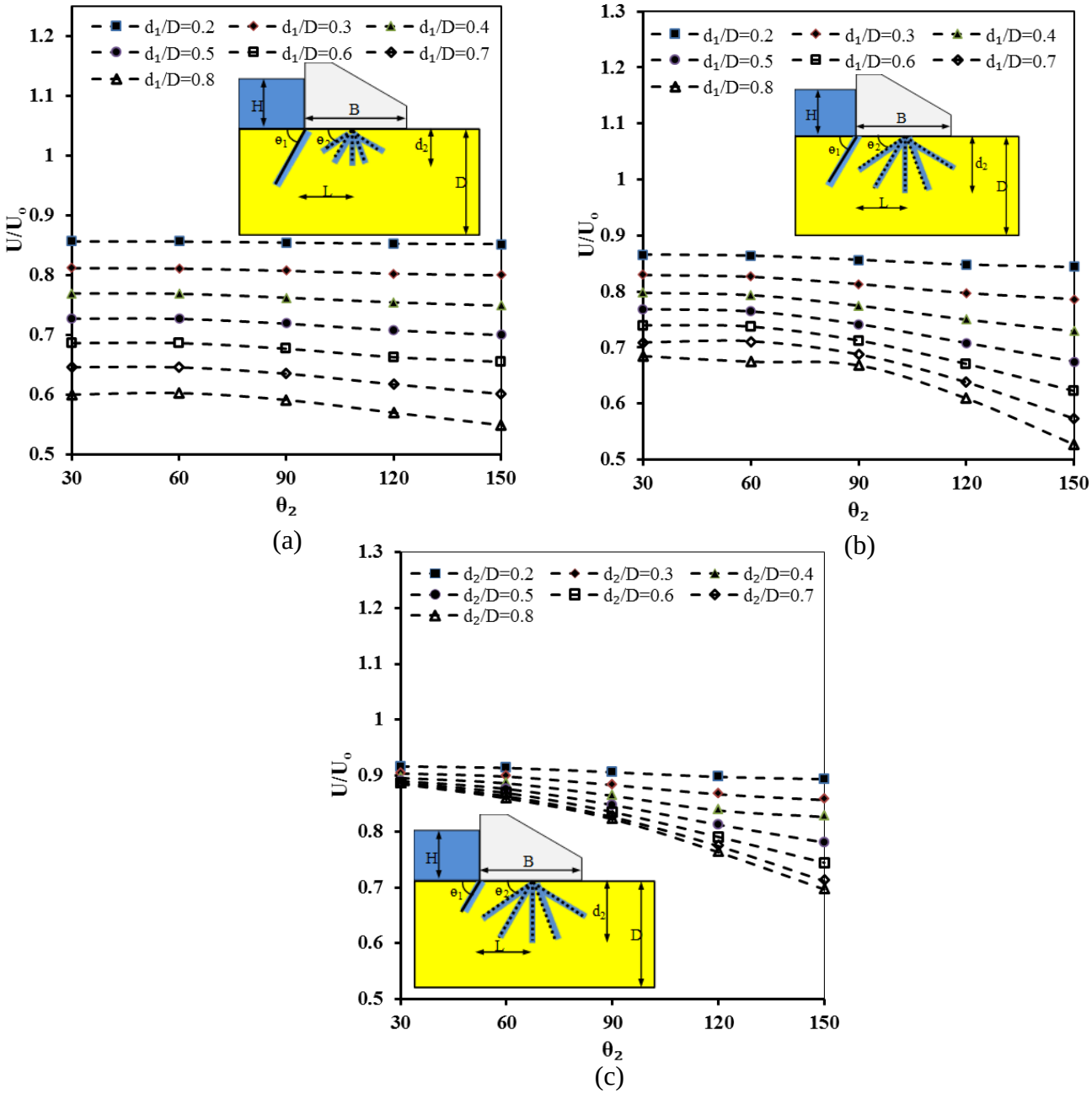

Fig. 9: Variation of the relative uplift force (U/U_o) with the inclination angle of the downstream cutoff wall (θ_2) for θ_1=60, L/B=0.5 and for d_2/d_1=0.5 (a), 1.0 (b), and 2.0 (c).

Fig.10 shows the variations of the relative uplift force (U/U_o) with the inclination angle of the downstream cutoff wall (θ_2) for $\theta_1 = 60^o$, $L/B = 1.0$ and for three cases of $d_2/d_1 = 0.5$, 1.0, and 2.0. For $d_2/d_1 = 0.5$, as the inclination angle θ_2 increases from 30° to 150°, a slight increase in the value of the relative uplift force U/U_o is observed (Fig. 10(a)). In Fig 10b, with increasing the relative depth of cutoff walls d_2/d_1 to 1.0, the value of U/U_o decreases with inclination angles θ_2 of 30° and 150°. In case of θ_2 equals to 60° and 120°, the resulting U seems to be constant at different relative cutoff wall depths. On the other hand, with d_2/d_1 =1.0, L/B = 1.0, and vertical downstream cutoff wall (θ_2 = 90°), the uplift force increases with increasing the relative depth of the upstream cutoff wall (d_1/D). For d_2/d_1=2.0 (Fig. 10c), increasing the relative depth d_2/D from 0.2 to 0.8, increases the relative uplift force U/U_o. The values of U/U_o are slightly higher for θ_2 = 90° compared to other inclination angles. Increasing the depth of the downstream cutoff wall d_2 more than d_1 (d_2/d_1=2.0) increases the uplift force compared to the case without cutoff wall.

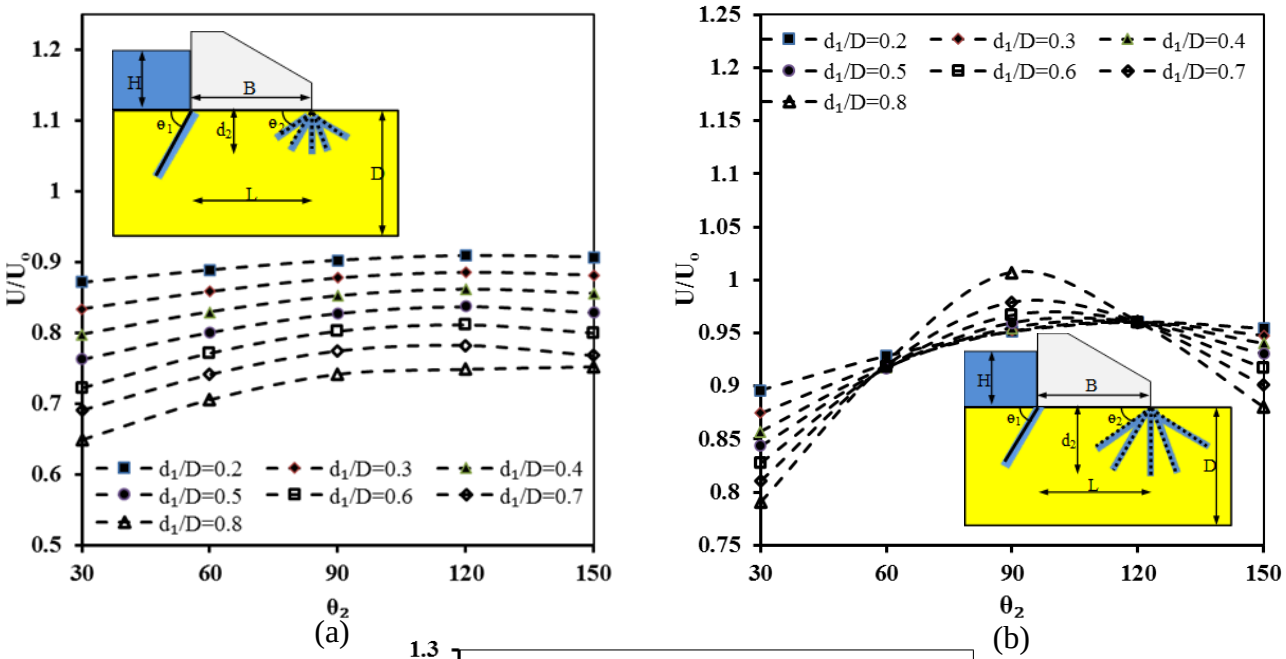

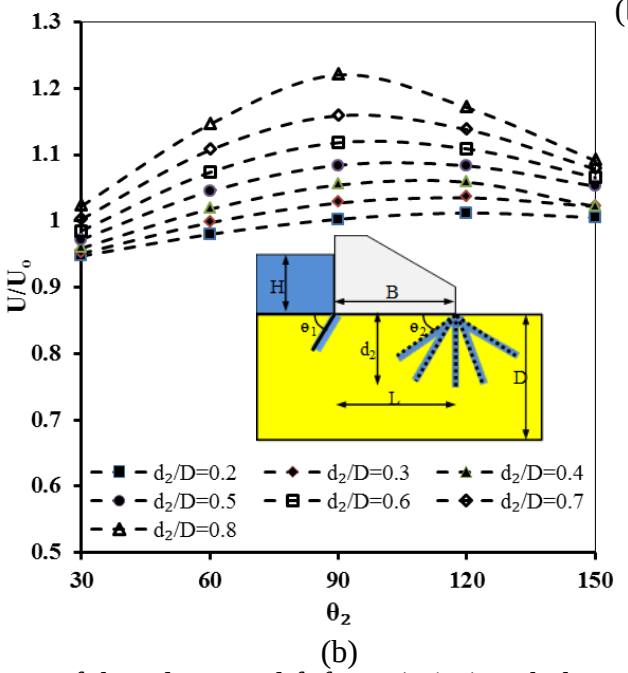

Fig. 10: The variation of the relative uplift force (U/U_o) with the inclination angle of the downstream cutoff wall (θ_2) for θ_1=60, L/B=1.0 and for d_2/d_1=0.5 (a), 1.0 (b), and 2.0 (c).

Fig. 11 is the same as Fig. 9 but for θ_1 = 90º. In case of d_2/d_1 = 0.5 (Fig. 11a), as d_2/D increases, U/U_o decreases but the variation is less significant than in the case of θ_1 = 60º (Fig. 9a). In case of d_2/d_1=1.0, as presented in Fig. 11.b, the value of U/U_o decreases with the increase of cutoff wall depths (d_1, d_2). The values of U/U_o remain constant for downstream cutoff wall inclination angles θ_2 of 30º, 60º, and 90º. As the value of θ_2 exceeds 90º, it causes a very little decrease in the resultant relative uplift force U/U_o. With d_2/d_1=2.0, (Fig. 11.c), U/U_o decreases with the increase of d_1 and d_2. In addition, for the same condition of d_2/d_1=2.0, and L/B=0.5, changing the inclination angle of the upstream wall θ_1 from 60º (Fig. 9.c) to θ_1=90 (Fig. 11.c) has no effect on the resultant values of U/U_o with different values of θ_2.

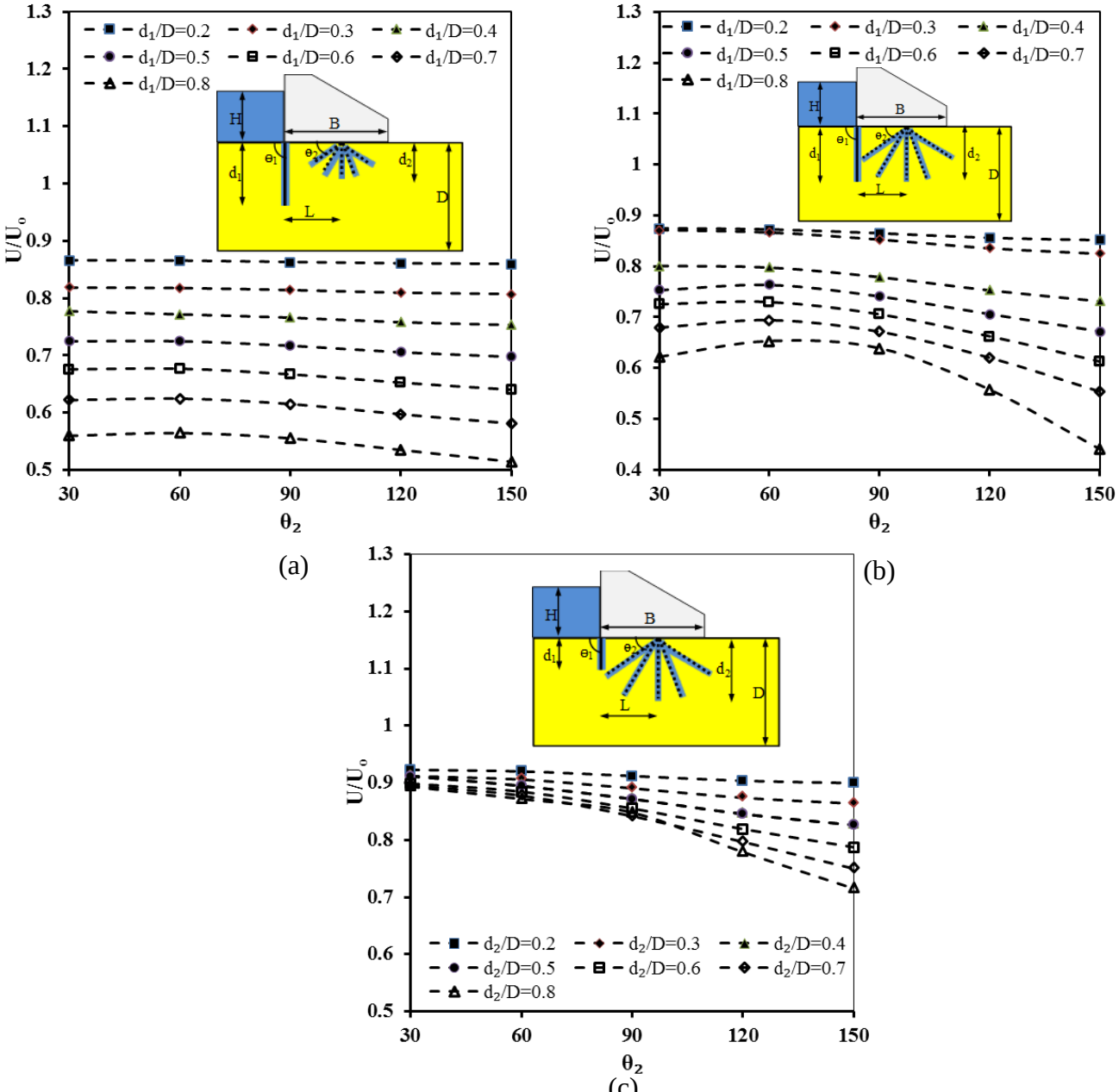

Fig. 11: Variation of relative uplift force (U/U_o) with the inclination angle of the downstream cutoff wall (θ_2) for θ_1=90, L/B=0.5 and for d_2/d_1=0.5 (a), 1.0 (b), and 2.0 (c).

Figure 12 shows the variation of the relative uplift force (U/U_o) with the inclination angle of the downstream cutoff wall (θ_2) for θ_1=90, L/B=1.0, for three cases of d_2/d_1=0.5, 1.0, and 2.0. Fig. 12.a shows that for d_2/d_1=0.5, increasing the depth of the upstream and downstream cutoff walls leads to decrease in the uplift force. With different values of θ_2, the values of U/U_o increase for with increasing θ_2 from 30° to 90°, while it still constant with values of θ_2 beyond 90° (120°, and 150°). Comparing with the results of Fig. 11.a, for the same condition of d_1 and d_2, the values of U/U_o with L/B=0.5 are slightly less than L/B=1.0 (Fig. 12.a). Fig. 12.b shows that, for equal depth of the upstream and downstream cutoff walls, with right angle upstream and downstream cutoff walls, the relative uplift force is constant (about 1.025) with different depths of d_1 and d_2. In addition,, the value of U/U_o decreases with increasing the upstream and downstream cutoff walls depth ratios d_1/D *and* d_2/D. This is valid with θ_2 values 30°, 60°, 120°, and 150°. Comparison of Figs. 12.a and 12.b shows that, the resultant U/U_o with equal depths of d_1 and d_2 (Fig. 12.b) is higher than U/U_o with d_2/d_1=0.5 (Fig 12.a). Fig 12.c shows that for d_2/d_1=2.0, U/U_o is higher than d_2/d_1=0.5 (Fig. 12.a) and d_2/d_1=1.0 (Fig. 12.b). The value of U/U_o increases with increasing the depth of the downstream cutoff wall. The value of U/U_o with θ_2=90° is higher than θ_2 equal to 30°, 60°, 120°, and 150°.

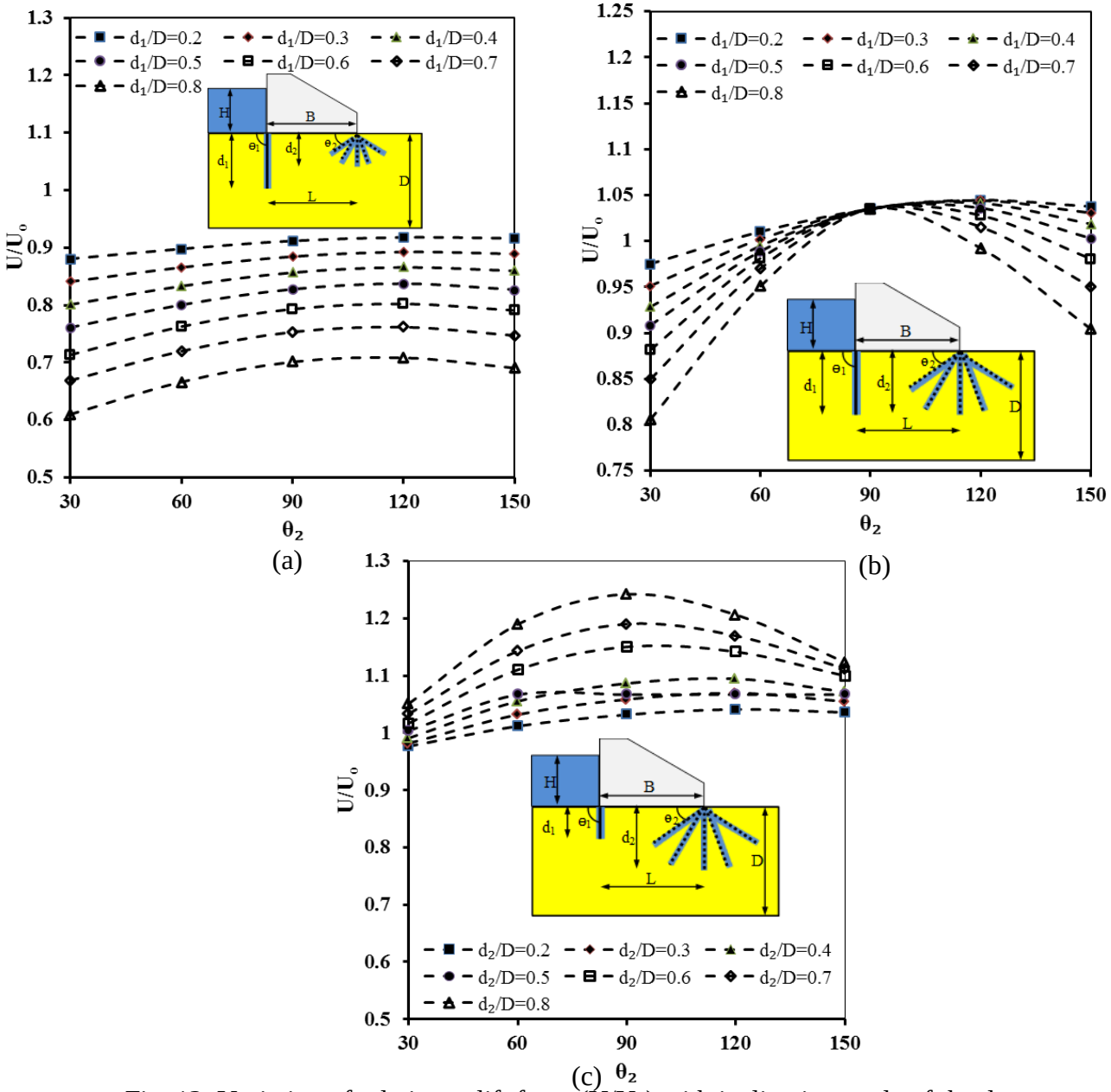

Fig. 12: Variation of relative uplift force (U/U_o) with inclination angle of the downstream cutoff wall (θ_2) for θ_1=90, L/B=1.0 and for d_2/d_1=0.5 (a), 1.0 (b), and 2.0 (c).

Figure 13 shows the variation of the relative uplift force (U/U_o) with the inclination angle of the downstream cutoff wall (θ_2) for θ_1=120, L/B=0.5, for three cases of d_2/d_1=0.5, 1.0, and 2.0. Fig. 13.a shows that for d_2/d_1=0.5, U/U_o is constant for different values of θ_2; the relative uplift U/U_o decreases with increasing the cutoff wall depths ratio. For with equal depth of cutoff walls, d_2/d_1=1.0, the relative uplift force U/U_o decreases with increasing the depth of the cutoff walls (Fig. 13b). In addition, the value of U/U_o decreases slightly with the increase of θ_2 from 30° to 150°. Fig 13.c shows that, for d_2/d_1=2.0, U/U_o decreases with the increase of upstream and downstream cutoff wall depths. Also, for θ_2 30° and 60° the value of U/U_o is nearly constant and with θ_2 more than 60°, the value of U/U_o decreases for different values of d_2/D.

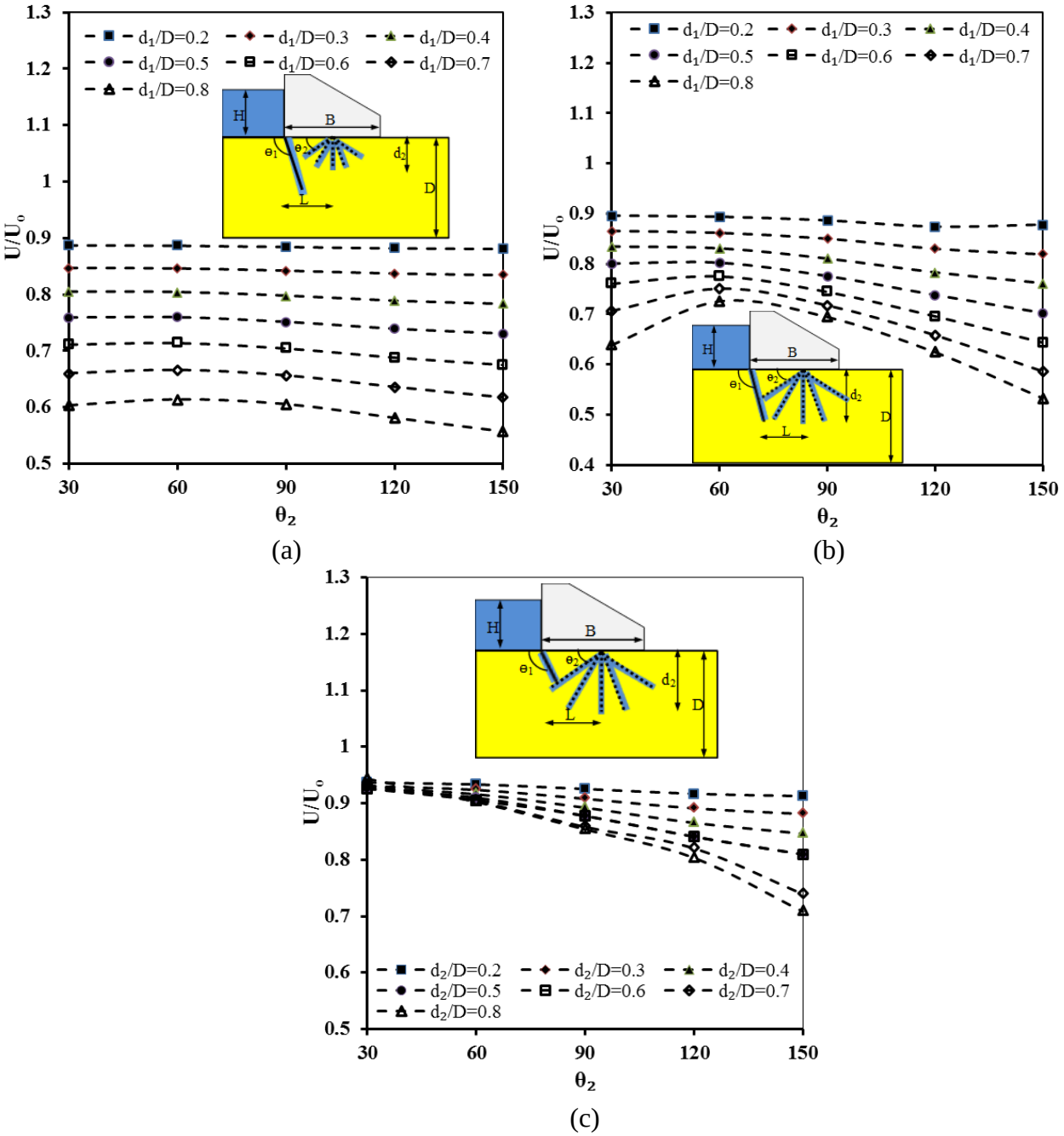

Fig. 13: Variation of relative uplift force (U/U_o) with inclination angle of the downstream cutoff wall (θ_2) for θ_1=120, L/B=0.5 and for d_2/d_1=0.5 (a), 1.0 (b), and 2.0 (c).

Figure 14 shows the variation of the relative uplift force (U/U_o) with the inclination angle of the downstream cutoff wall (θ_2) for θ_1=120, and L/B=1.0, for three cases of d_2/d_1=0.5, 1.0, and 2.0. Fig 14.a indicates that for d_2/d_1=0.5, the values of U/U_o increase with increase of θ_2, but for θ_2 more than 90°, U/U_o remains constant. In addition, U/U_o decreases with increasing the cutoff wall depths. Fig 14.b shows that for d_2/d_1=1.0, the values of U/U_o is nearly constant with different depths d_2/D and θ_2 equal to 60° and 120°. With θ_2 equal to 30° and 150°, increasing the depth of downstream cutoff wall d_2/D causes decrease in U/U_o. On the other hand, U/U_o increases with the increase of d_2/D, in case of vertical downstream cutoff wall. Decreasing the depth of the downstream cutoff wall (d_2/d_1=0.5) (Fig. 14.a) results in lower U/U_o compared with d_2/d_1=1.0 and 2.0 as shown in Fig. 14 b and c respectively.

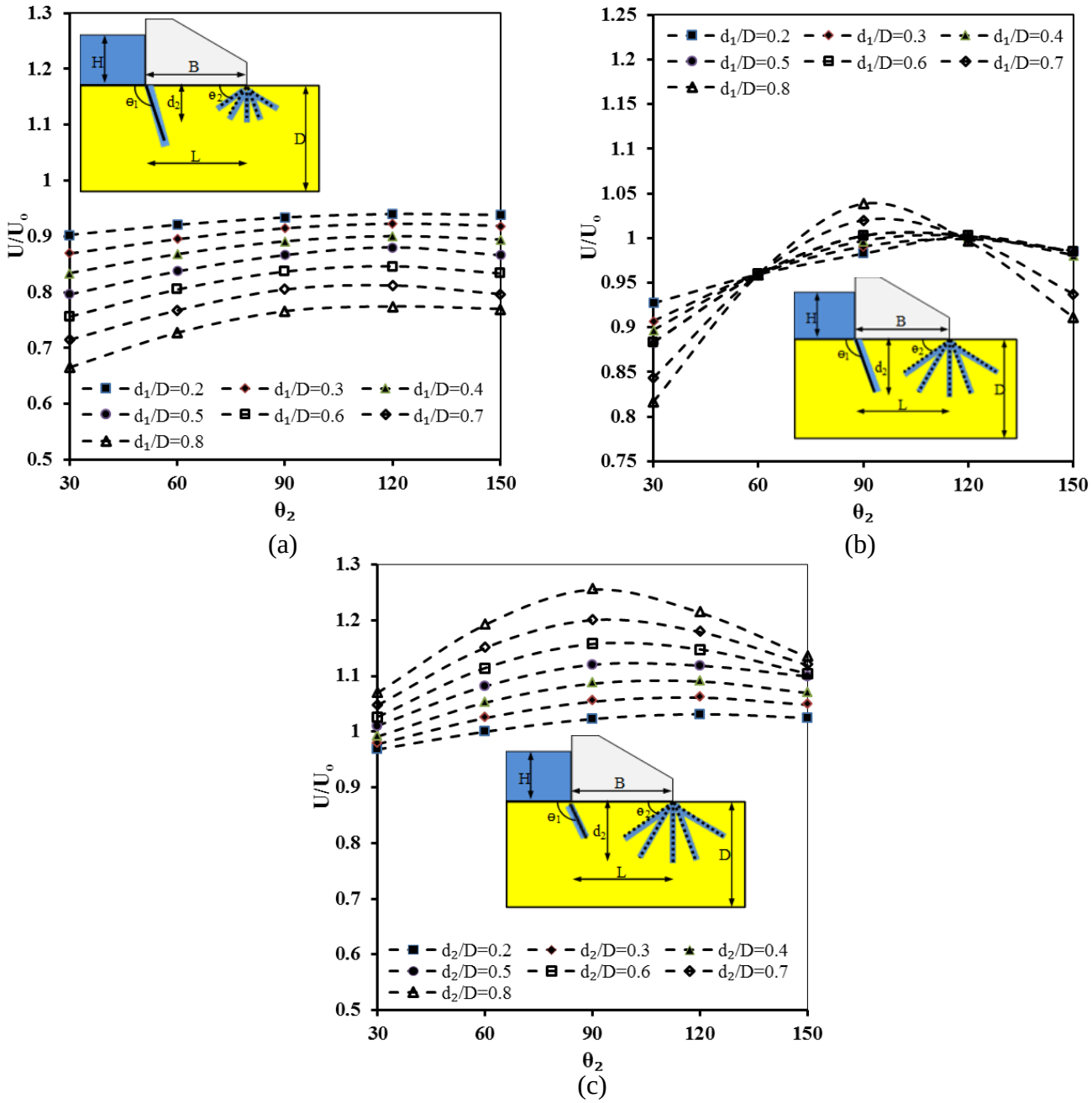

Fig. 14: Variation of relative uplift force (U/U_o) with inclination angle of the downstream cutoff wall (θ_2) for θ_1=120, L/B=1.0 and for d_2/d_1=0.5 (a), 1.0 (b), and 2.0 (c).

Effectiveness of inclined double cutoff walls in controlling the exit hydraulic gradient:

Figure 15 presents the variations of the relative exit hydraulic gradient (i/i_o) with the inclination angle of the downstream cutoff wall (θ_2) for θ_1=60 and L/B=0.5, for three cases of cutoff wall depth ratios d_2/d_1=0.5, 1.0, and 2.0. Fig. 15(a) shows that for d_2/d_1=0.5, the exit hydraulic gradient decreases with increasing the depths of the upstream and downstream cutoff walls (d_1 and d_2). In addition, with increasing θ_2, the resulting exit hydraulic gradient is relatively constant and there is a very slight variation in i/i_o. Fig. 15(b) shows that for d_2/d_1=1.0, with increasing the depths (d_1 and d_2), the values of i decreased. Furthermore, with increasing (θ_2) from 30° to 90°, the resulting i is slightly decreased with a very slight variation in i/i_o. By increasing θ_2 beyond 90°, the exit hydraulic gradient increases. For d_2/d_1=2.0, it is seen that increasing the depth of the cutoff walls (d_1 and d_2) results in decrease in the exit hydraulic gradient, and the value of i is lower with θ_2 = 90° compared with 30°, 60°, 120°, and 150° (Fig. 15c).

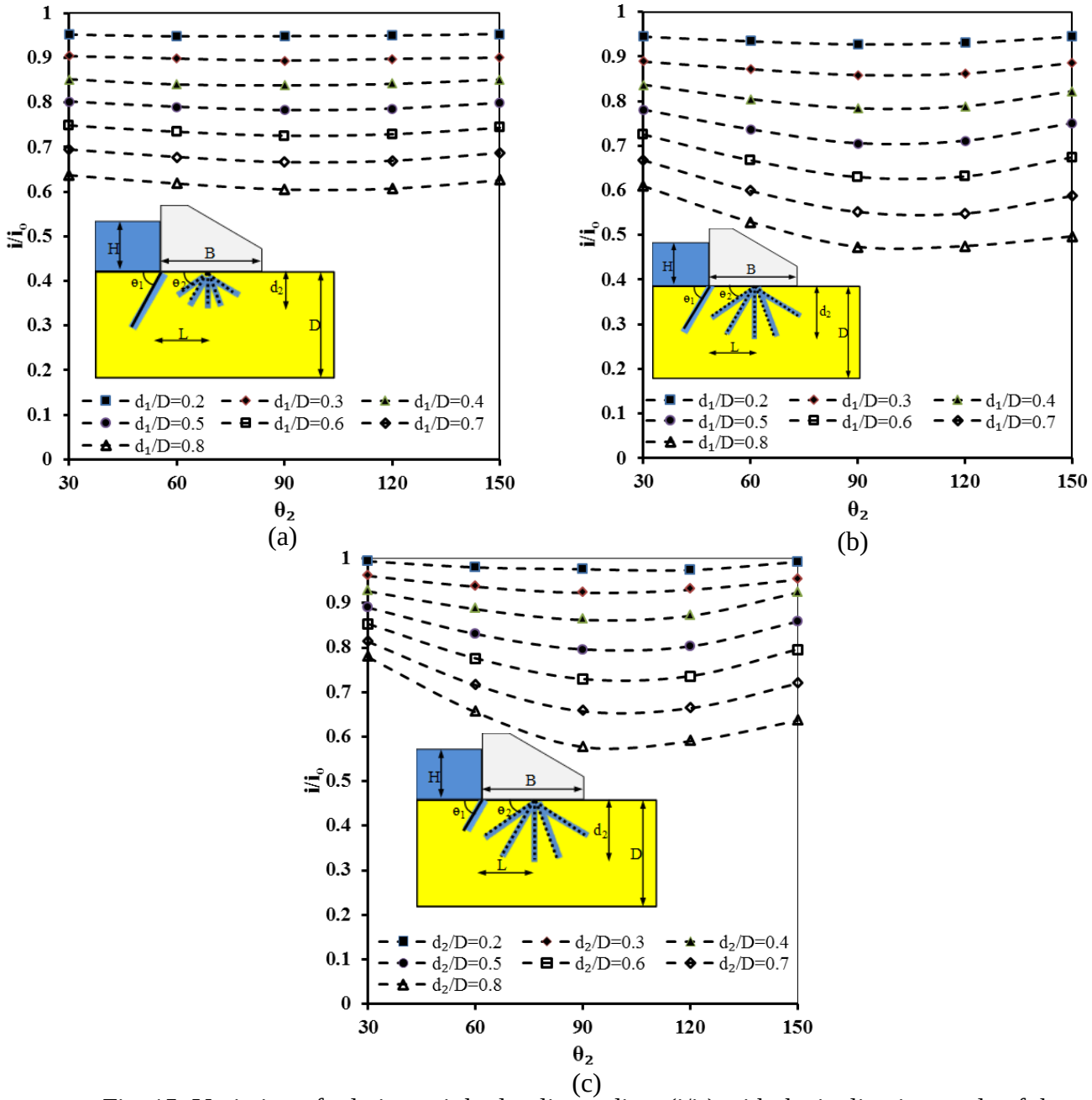

Fig. 15: Variation of relative exit hydraulic gradient (i/i_0) with the inclination angle of the downstream cutoff wall (θ_2) for θ_1=60°, L/B=0.5 and for d_2/d_1=0.5 (a), 1.0 (b), and 2.0 (c).

Figure 16 shows the same of Fig 15 but for L/B=1.0. For d_2/d_1=0.5, the values of exit hydraulic gradient decrease with increasing d_1 and d_2 (Fig 16.a). In addition, increasing the inclination angle θ_2 from 30° to 150°, results in a rapid reduction on the value of relative exit gradient i/i_o. With increasing the relative depth of the cutoff walls d_2/d_1 to 1.0, the value of i/i_o decreases slightly compared with d_2/d_1=0.5 (Fig 16.b). For d_2/d_1=2.0 (Fig. 16.c) increasing the relative depth d_2/D from 0.2 to 0.8, leads to decrease in the relative exit hydraulic gradient i/i_o. The value of i/i_o is slightly higher in the case of d_2/d_1=2.0 compared with d_2/d_1=0.5 and d_2/d_1=1.0 for different inclination angles. It should be noted that the exit hydraulic gradient decreases more when the downstream cutoff wall is installed in the end with L/B=1.0 compared with L/B=0.5 (Fig 15). The relative exit hydraulic gradient (i/i_o) can be decreased to less than 0.25 with θ_2 more than 90°. The results (Fig. 16) confirm that the slope of the relative exit gradient curves decrease rapidly with increasing θ_2 from 30° to 150° for different ratios d_2/d_1.

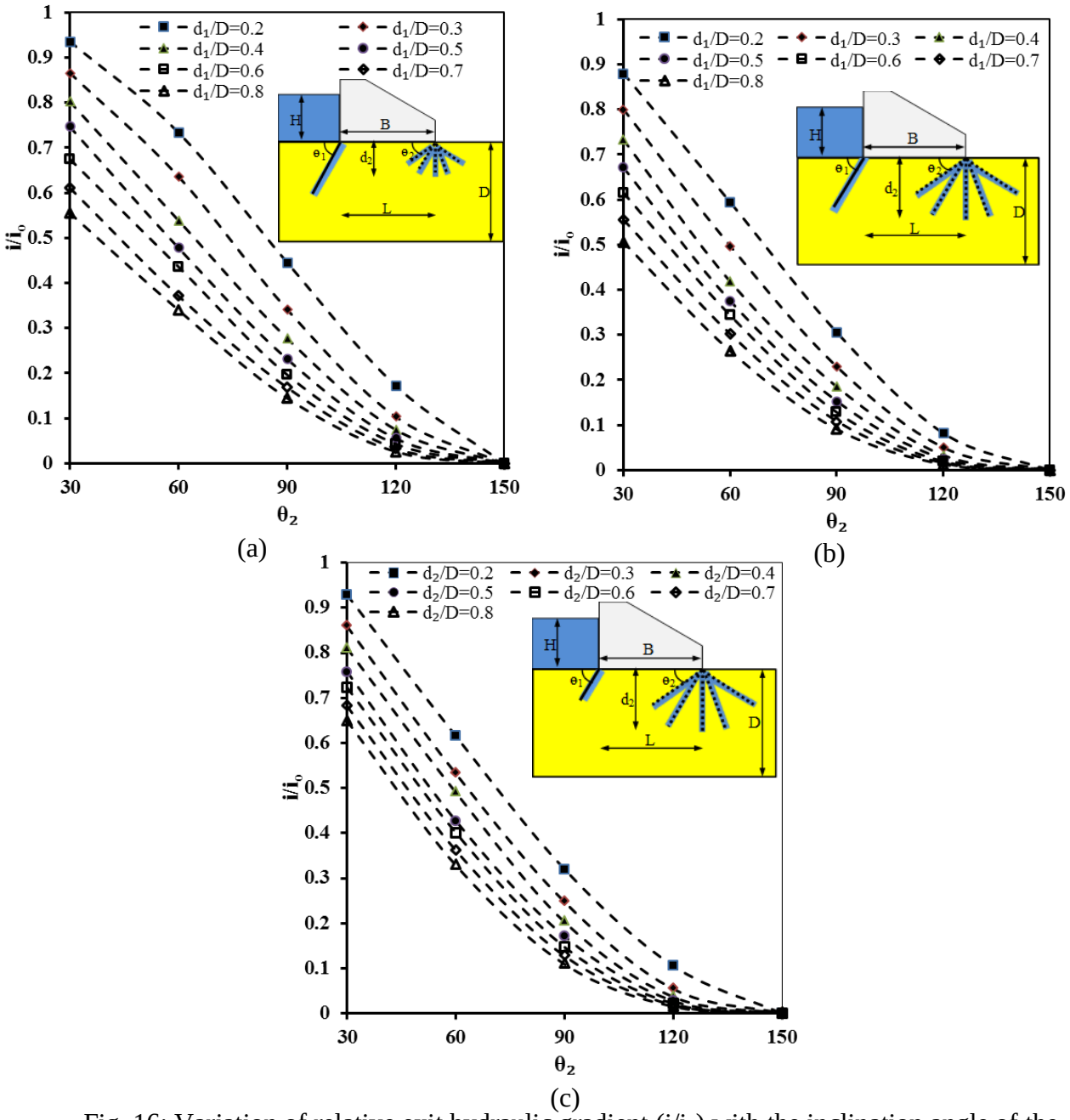

Fig. 16: Variation of relative exit hydraulic gradient (i/i_o) with the inclination angle of the downstream cutoff wall (θ_2) for θ_1=60°, L/B=1.0 and for d_2/d_1=0.5 (a), 1.0 (b), and 2.0 (c).

Figure 17 shows the variation of the relative exit hydraulic gradient (i/i_o) with the inclination angle of the downstream cutoff wall (θ_2) for θ_1=90° and L/B=0.5, for three cases of d_2/d_1=0.5, 1.0, and 2.0. In case of d_2/d_1=0.5, as shown in Fig. 11.a, with increasing d_1/D, the i/i_o values decreasing, very little decreasing in the result relative i/i_o produces with θ_1=90° in Fig. 17.a compared with θ_1=60° (Fig. 15.a). In case of d_2/d_1=1.0, as presented in Fig. 17.b, the values of i/i_o decrease with the increase of cutoff wall depths (d_1, d_2). In addition, the values of i/i_o results in a decrease with increasing the inclination angle θ_2 from 30° to 90°. Also, with values of θ_2 exceeds 90°, cause a very little increase in the resultant relative value of exit gradient i/i_o. As shown in Fig. 17.c, with d_2/d_1=2.0, i/i_o decreases with the increase of d_1 and d_2. In addition, changing the values of θ_1 from 60° (Fig. 15.c) to θ_2=90 (Fig. 17.c) has little effect on decreasing the resultant values of i/i_o with the same conditions of d_1, d_2, and L/B=0.5.

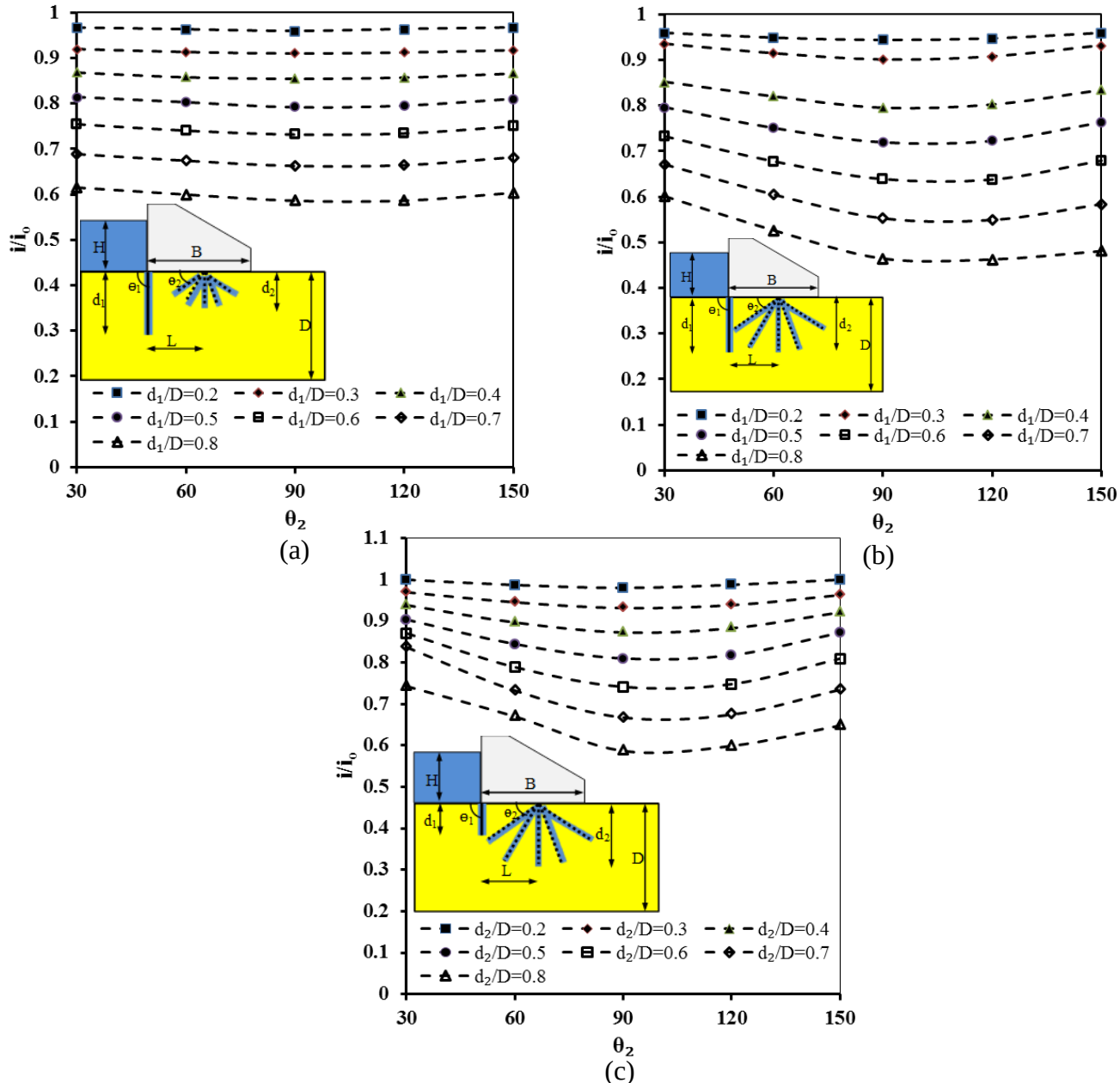

Fig. 17: Variation of relative exit hydraulic gradient (i/i_o) with the inclination angle of the downstream cutoff wall (θ_2) for θ_1=90°, L/B=0.5 and for d_2/d_1=0.5 (a), 1.0 (b), and 2.0 (c).

Figure 18 presents the variation of (i/i_o) with the inclination angle (θ_2) for θ_1=90 and L/B=1.0, for three cases of d_2/d_1=0.5, 1.0, and 2.0. Fig. 18.a shows that for d_2/d_1=0.5, increasing the depths of d_1 and d_2 leads to decrease in the exit hydraulic gradient; i/i_o decreases rapidly with the increase of θ_2 from 30° to 150°. Fig. 18.b shows that for equal depths d_1 and d_2, with the upstream and downstream cutoff walls installed at right angle, increasing θ_2 results in a rapid reduction in relative exit hydraulic gradient. In addition, the value of i/i_o decreases with the increase of the depth ratio d_2/D. Comparison of the results in Figs. 18.a and 18.b shows that with equal depths of d_1 and d_2 (Fig. 18.b) the resultant relative i/i_o is less than with d_2/d_1=0.5 (Fig 18.a). Fig 12.c shows that for d_2/d_1=2.0, the value of i/i_o is higher than d_2/d_1=0.5 (Fig. 18.a) and d_2/d_1=1.0 (Fig. 18.b). i/i_o increases with increasing the depths of the cutoff walls; the value of i/i_o is less than 0.10 with θ_2 =120° and 150°. The slope of the exit hydraulic gradient curves for different ratios d_2/d_1=0.5, 1.0, and 2.0 demonstrates a rapid reduction with increasing θ_2 from 30° to 150°.

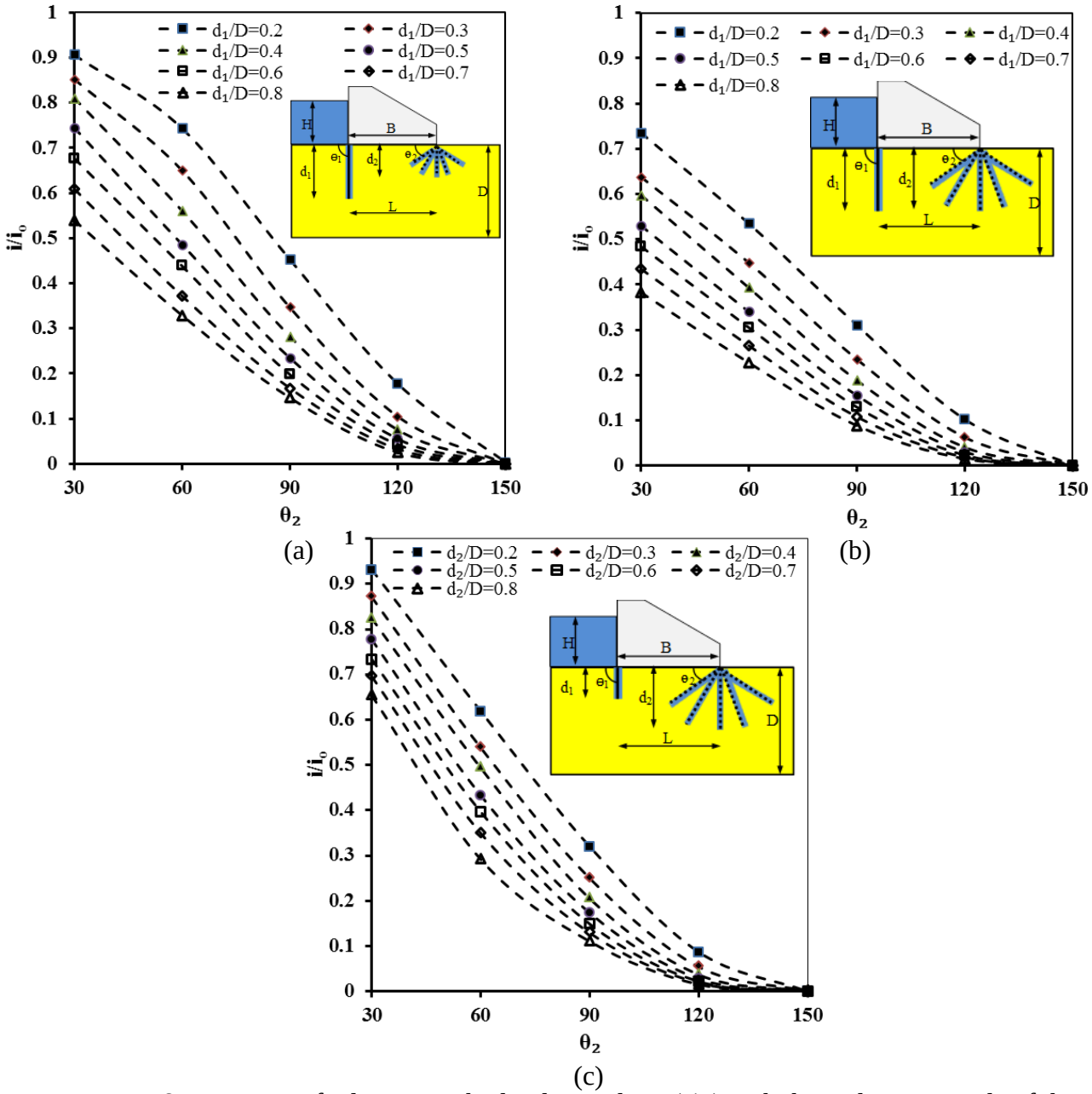

Fig. 18: Variation of relative exit hydraulic gradient (i/i_o) with the inclination angle of the downstream cutoff wall (θ_2) for θ_1=90°, L/B=1.0 and for d_2/d_1=0.5 (a), 1.0 (b), and 2.0 (c).

Figure 19 introduces the variation of the relative exit hydraulic gradient (i/i_o) with the inclination angle of the downstream cutoff wall (θ_2) for θ_1=120 and L/B=0.5, for three cases of d_2/d_1=0.5, 1.0, and 2.0. Fig. 19.a shows that for d_2/d_1=0.5, the values of i/i_o are nearly constant for different values of θ_2. In addition, the value of i/i_o decreases with the increase of cutoff wall depths ratio. Fig 19.b indicates that for d_2/d_1=1.0 (equal depth of cutoff walls), i/i_o decreases with the increase of the cutoff wall depths. In addition, the value of i/i_o decreases slightly with the increase of θ_2 from 30° to 150°. For d_2/d_1=2.0, i/i_o decreases with increasing the depths of the upstream and downstream cutoff walls (Fig 19.c). For θ_2 = 30° and 60° the value of i/i_o is nearly constant and with θ_2 more than 60°, i/i_o decreases for different values of d_2/D.

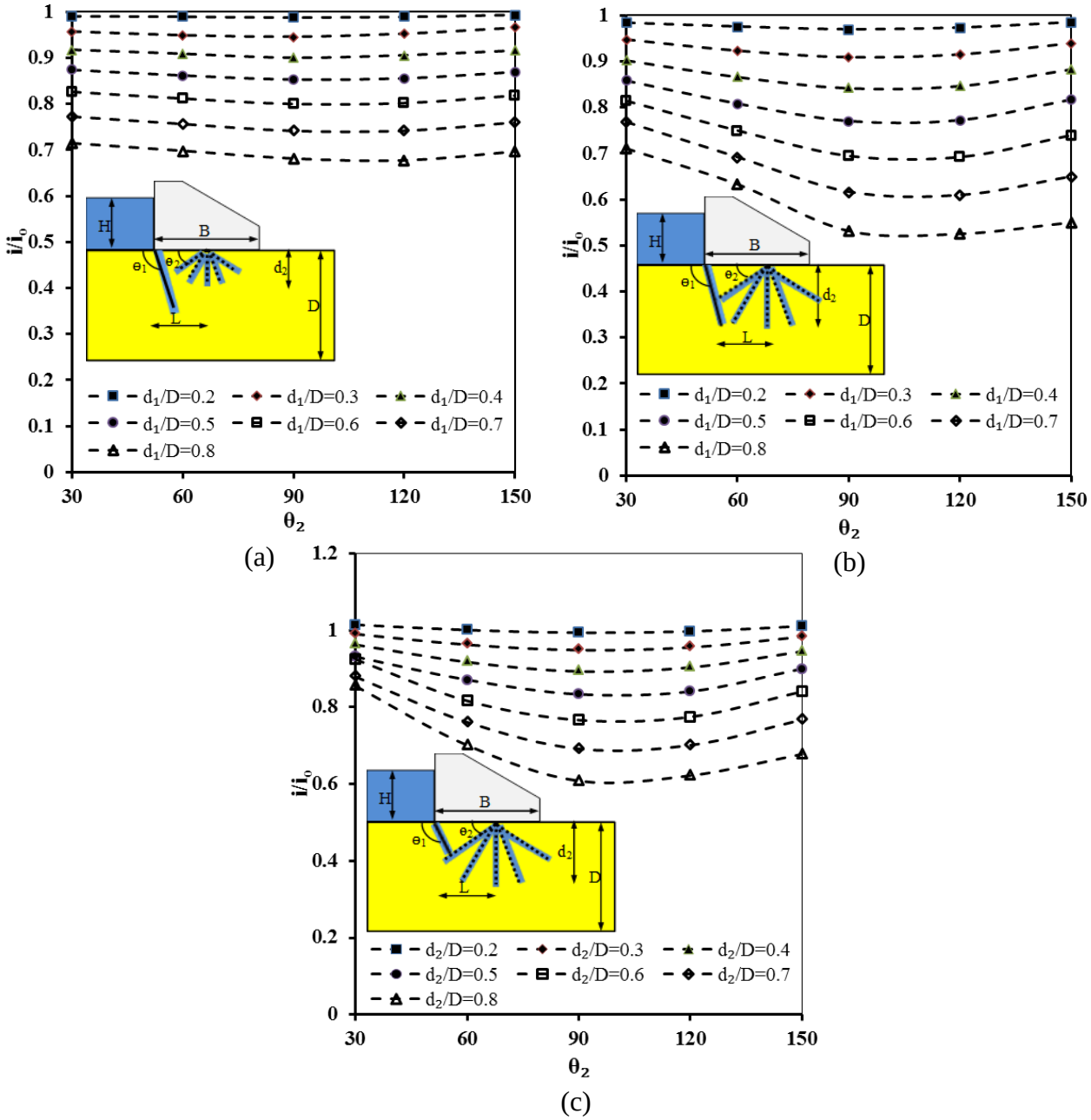

Fig. 19: Variation of relative exit hydraulic gradient (i/i_o) with the inclination angle of the downstream cutoff wall (θ_2) for θ_1=120°, L/B=0.5 and for d_2/d_1=0.5 (a), 1.0 (b), and 2.0 (c).

Figure 20 shows the variation of (i/i_o) with the inclination angle (θ_2) for θ_1=120 and L/B=1.0 for three cases of d_2/d_1=0.5, 1.0, and 2.0. Figure 20 shows the same results as Figure 13 but for L/B=1.0. Fig 20.a shows that for d_2/d_1=0.5, the i/i_o decreases with the increase of θ_2. In addition, the value of i/i_o decreases with increasing the cutoff wall depths. The slope of relative exit hydraulic gradient shows a rapid reduction with increasing θ_2 from 30° to 150° for different depth ratios d_2/d_1=0.5, 1.0 and 2.0. Fig 20.b shows that for d_2/d_1=1.0, the increase of cutoff wall depths results in a decrease of i/i_o values. The results confirmed that with (d_2/d_1=1.0) (Fig. 20.b) values of relative i/i_o are less compared with d_2/d_1=0.5 and 2.0 as shown in Fig. 20 a and c respectively. Installing the cutoff wall at the downstream end point with (L/B=1.0) results in minimization and controlling of relative exit hydraulic gradient i/i_o.

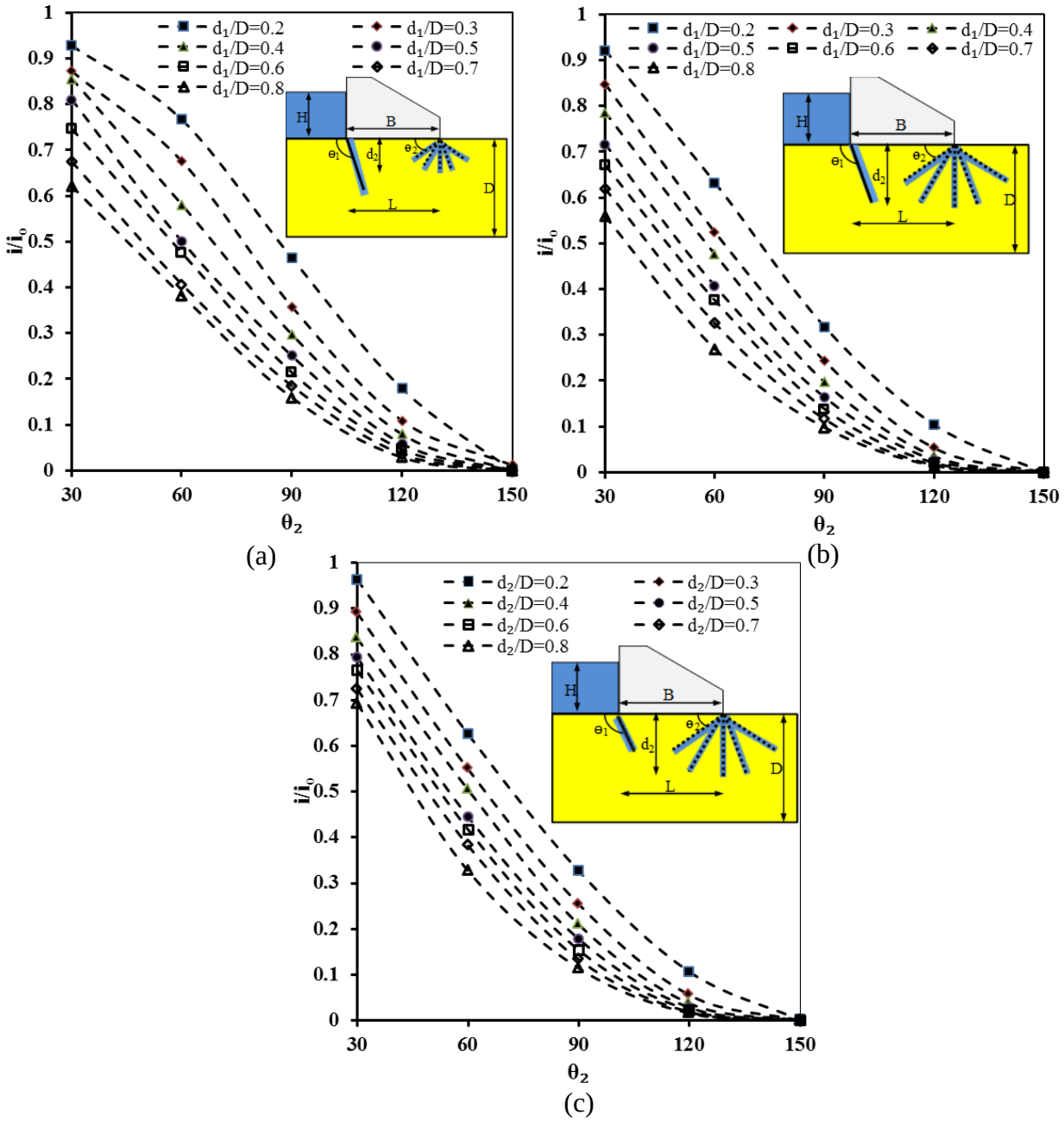

Fig. 20: Variation of relative exit hydraulic gradient (i/i_o) with the inclination angle of the downstream cutoff wall (θ_2) for θ_1=120°, L/B=1.0 and for d_2/d_1=0.5 (a), 1.0 (b), and 2.0 (c).

Effectiveness of inclined double cutoff walls in controlling the seepage discharge:

Figure 21 presents the variations of the relative seepage discharge (Q/Q_o) with the inclination angle of the downstream cutoff wall (θ_2) for θ_1=60, L/B=0.5 and three cases of cutoff wall depth ratios d_2/d_1=0.5, 1.0, and 2.0. Fig. 21(a) shows that for d_2/d_1=0.5, the seepage discharge decreases with increasing the depths of the upstream and downstream cutoff walls (d_1 and d_2). In addition, with increasing the inclination angle of the downstream cutoff wall (θ_2), the resulting seepage discharge is relatively constant and Q/Q_o varies very slightly. Fig. 21(b) shows that for d_2/d_1=1.0, with increasing the depths (d_1 and d_2), the values of Q decrease. In addition, with increasing (θ_2) from 30° to 90°, the resulting Q is slightly decreased and a very slight variation occurs in Q/Q_o. By increasing θ_2 beyond 90°, the seepage discharge increases. For d_2/d_1=2.0, increasing the depth of the cutoff walls (d_1 and d_2) results in a decrease in the seepage discharge (Fig. 21c), while the value of Q deceases more with θ_2 equal to 90° compared with 30°, 60°, 120°, and 150°.

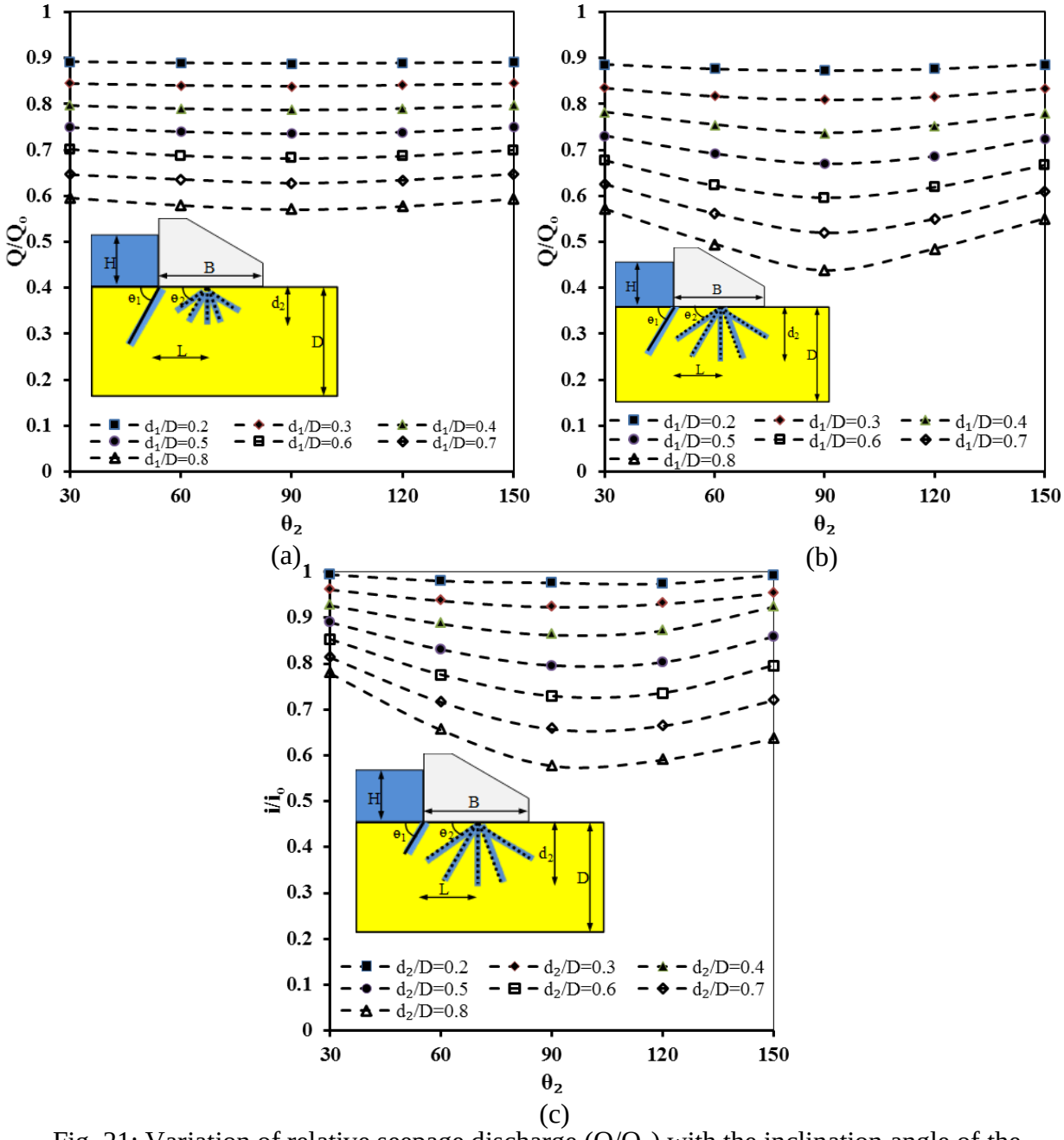

Fig. 21: Variation of relative seepage discharge (Q/Q_o) with the inclination angle of the downstream cutoff wall (θ_2) for θ_1=60°, L/B=0.5 and for d_2/d_1=0.5 (a), 1.0 (b), and 2.0 (c).

Figure 22 shows similar results as Fig 21 but for L/B=1.0. For d_2/d_1=0.5 (Fig 22.a) the seepage discharge decreases with the increase of d_1 and d_2. In addition, increasing the inclination angle θ_2 from 30° to 150°, results in a slight reduction in the value of seepage discharge ratio Q/Q_o. With increasing the relative depth of the cutoff walls d_2/d_1 to 1.0, the value of Q/Q_o decreases slightly compared with d_2/d_1=0.5 (Fig 22.b). For d_2/d_1=2.0, increasing the relative depth d_2/D from 0.2 to 0.8, leads to decrease in the relative seepage discharge Q/Q_o (Fig. 22.c). The value of Q/Q_o is slightly higher in case of d_2/d_1=2.0 compared with d_2/d_1=0.5 and d_2/d_1=1.0 for different inclination angles. The seepage discharge decreases more when the downstream cutoff wall is installed in the end with L/B=1.0 compared with L/B=0.5 (Fig 21). The results in Fig. 22 confirm that the relative seepage discharge ratio (Q/Q_o) decreases slightly with L/B=1.0 compared with L/B=0.50.

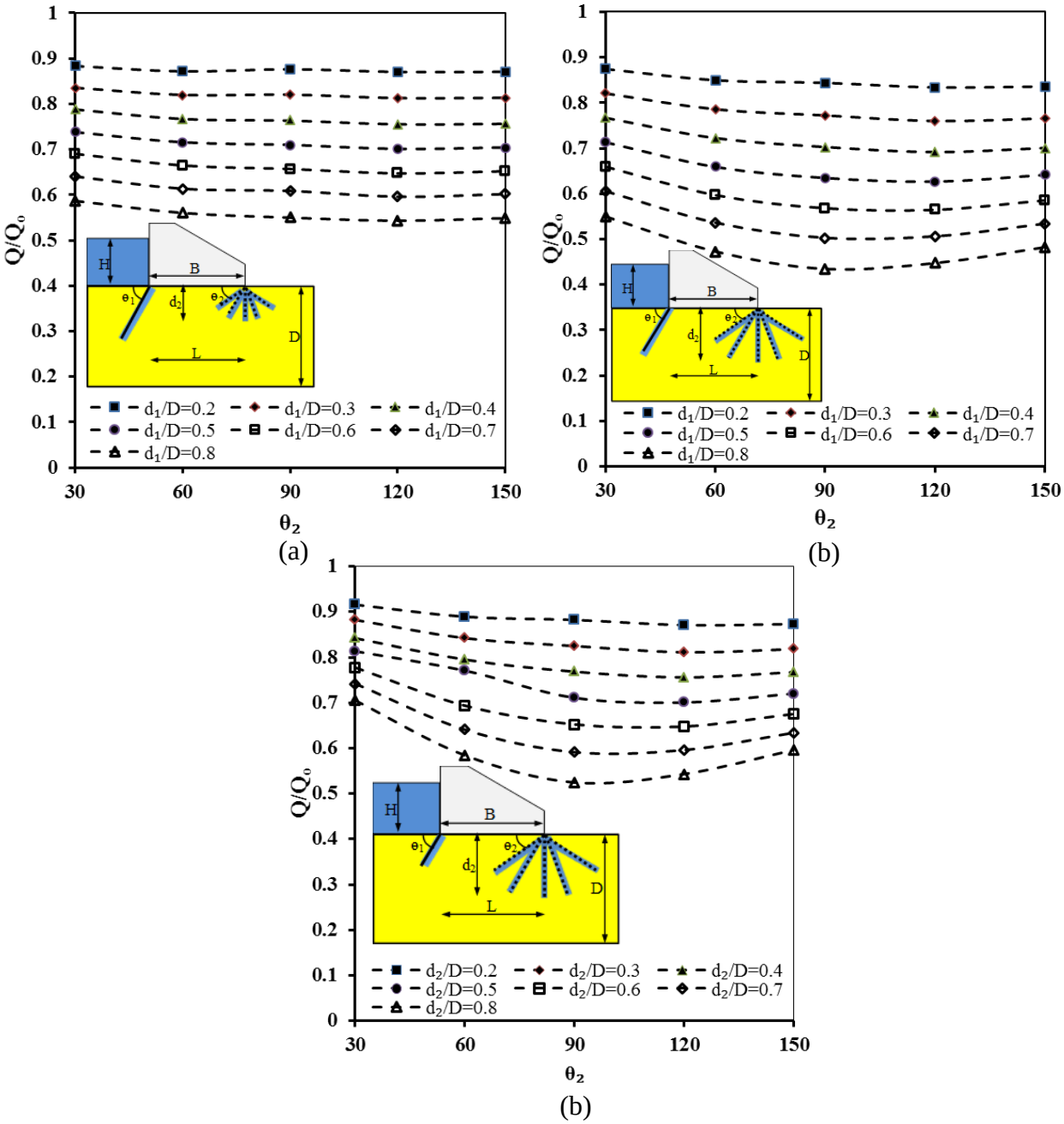

Fig. 22: Variation of relative seepage discharge (Q/Q_o) with the inclination angle of the downstream cutoff wall (θ_2) for θ_1=60°, L/B=1.0 and for d_2/d_1=0.5 (a), 1.0 (b), and 2.0 (c).

Figure 23 shows similar results as Fig. 20 but for θ_1=90°. In case of d_2/d_1=0.5, Q/Q_o decreases with increasing d_1/D. Very slight decrease is observed in the resultant relative Q/Q_o with θ_1=90° (Fig. 23.a) compared with θ_1=60° (Fig. 20.a). In case of d_2/d_1=1.0 (Fig. 23.b), Q/Q_o decreases with the increase of cutoff wall depths (d_1, d_2). The increase of the inclination angle θ_2 from 30° to 90° results in a reduction in the value of Q/Q_o. Also, the values of θ_2 higher than 90°, cause very little increase in the resultant relative seepage discharge Q/Q_o. With d_2/d_1=2.0 (Fig. 23.c), Q/Q_o decreases with the increase of d_1 and d_2. In addition, changing the values of θ_1 from 60° (Fig. 21.c) to θ_1=90 (Fig. 23.c) has little effect on the values of Q/Q_o with the same condition of d_1, d_2, and L/B=0.5.

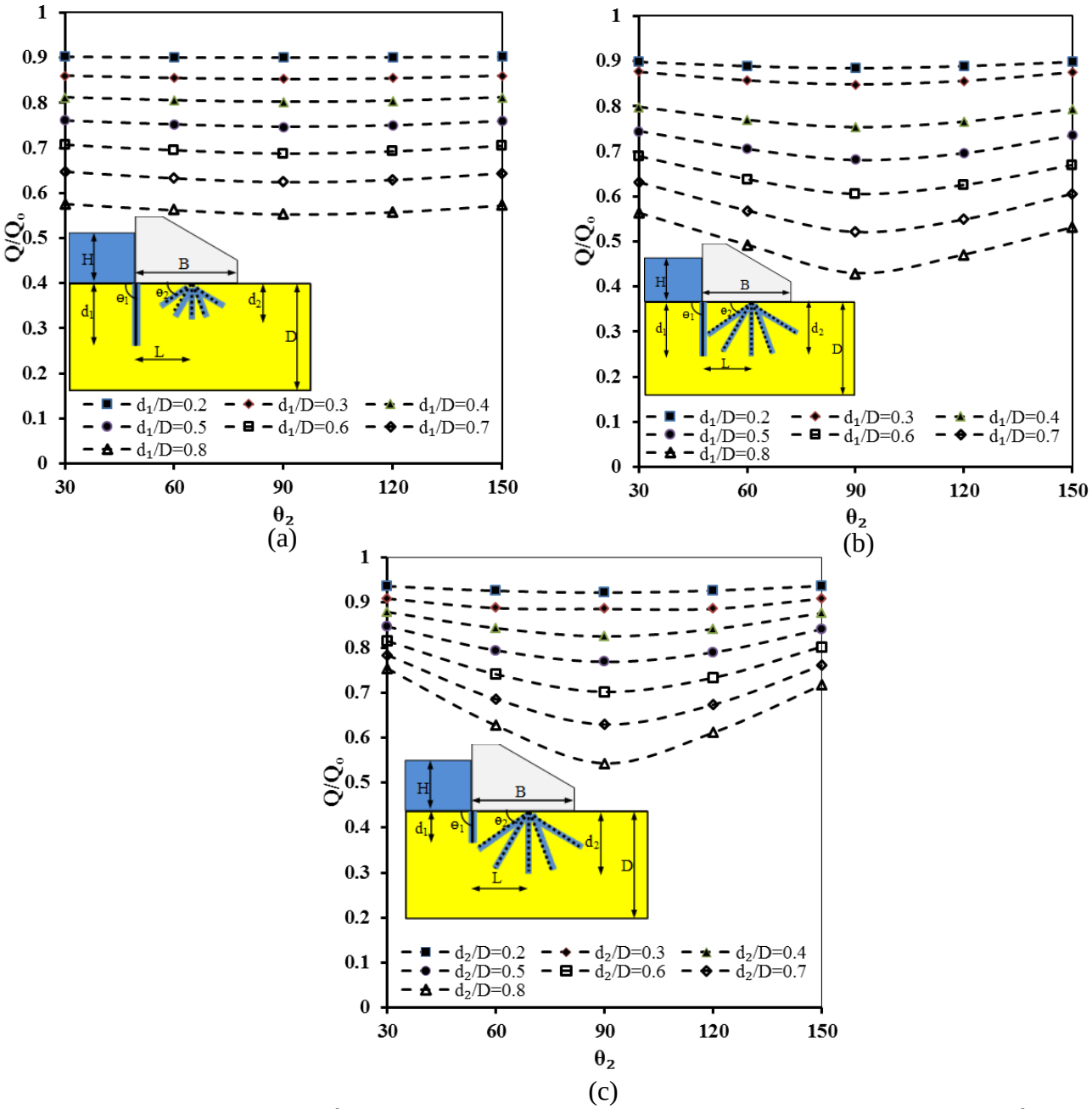

Fig. 23: Variation of relative seepage discharge (Q/Q_o) with the inclination angle of the downstream cutoff wall (θ_2) for θ_1=90°, L/B=0.5 and for d_2/d_1=0.5 (a), 1.0 (b), and 2.0 (c).

Figure 24 presents the variation of (Q/Q_o) with the inclination angle (θ_2) for θ_1=90 and L/B=1.0 for three cases of d_2/d_1=0.5, 1.0, and 2.0. Fig. 24.a shows that for d_2/d_1=0.5, increasing the depths of d_1 and d_2 leads to decrease in the seepage discharge. The values of Q/Q_o decrease slightly with the increase of θ_2 from 30° to 150°. Fig. 24.b shows that for equal depths of the upstream and downstream cutoff walls (d_1=d_2), increasing θ_2 results in a very slight reduction in relative seepage discharge. In addition, the value of Q/Q_o decreases with increasing the depth ratio d_2/D. Comparison of Figs. 24.a and 24.b reveals that with equal depth of d_1 and d_2 (Fig. 24.b), the resultant relative Q/Q_o is slightly less than with d_2/d_1=0.5 (Fig 24.a). The resultant relative discharge Q/Q_o with d_2/d_1=2.0 (Fig 24.c) is relatively higher than the cases of d_2/d_1=0.5 and d_2/d_1=1.0 (Fig. 24.a and 24.b respectively).

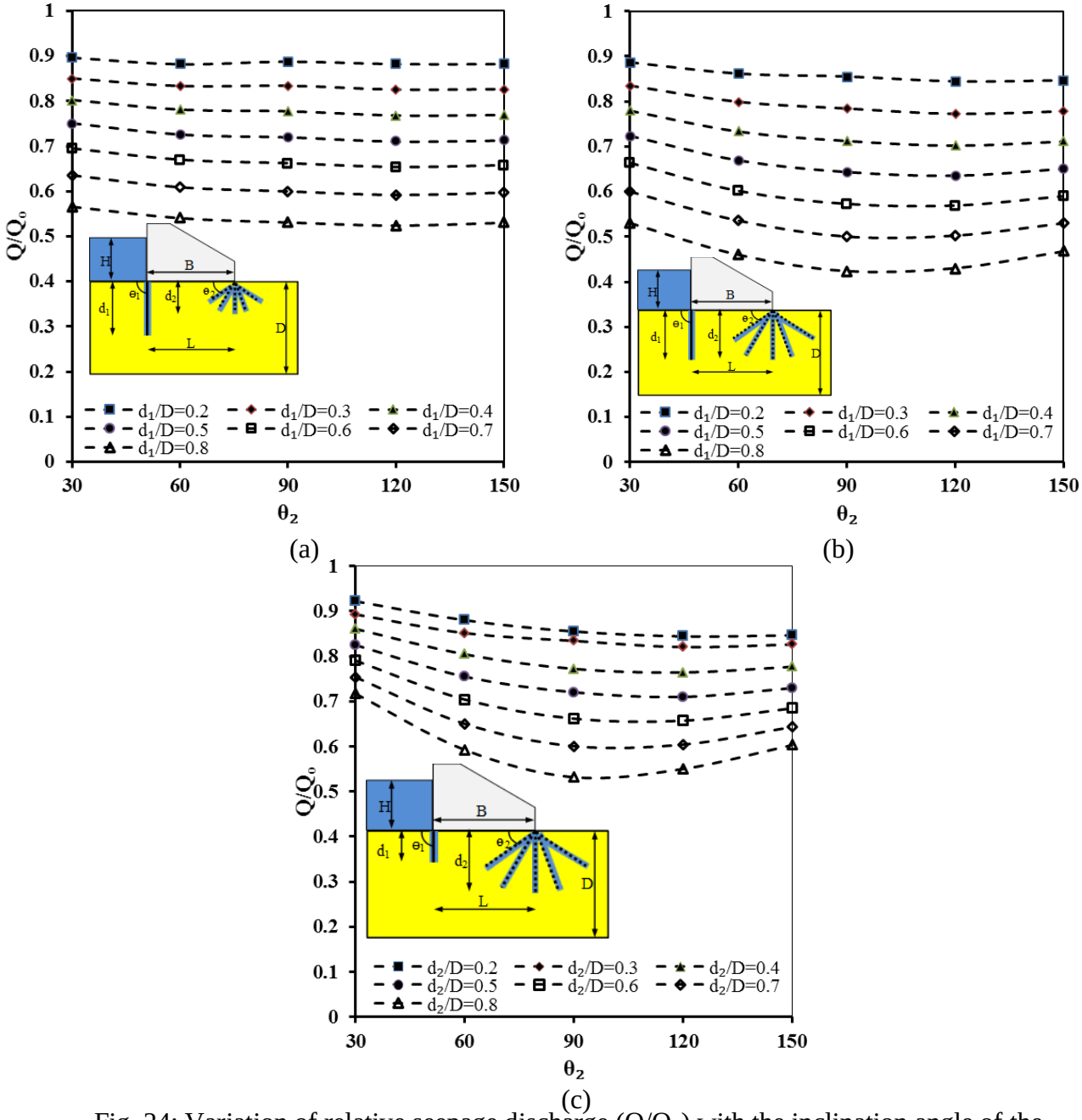

Fig. 24: Variation of relative seepage discharge (Q/Q_o) with the inclination angle of the downstream cutoff wall (θ_2) for θ_1 =90°, L/B=1.0 and for d_2/d_1=0.5 (a), 1.0 (b), and 2.0 (c).

Figure 25 introduces the variation of the relative seepage discharge (Q/Q_o) with the inclination angle of the downstream cutoff wall (θ_2) for θ_1=120 and L/B=0.5, for three cases of d_2/d_1=0.5, 1.0, and 2.0. Fig. 25.a shows that for d_2/d_1=0.5, the values of Q/Q_o are nearly constant for different values of θ_2. The relative seepage discharge Q/Q_o decreases with the increase of the cutoff wall depth ratios. Fig 25.b shows that for d_2/d_1=1.0, with equal depth of cutoff walls, Q/Q_o decreases with the increase of cutoff wall depths. In addition, the value of Q/Q_o decreases slightly with the increase of θ_2 from 30° to 90° ad then increases slightly when the value of θ_2 increases from 90° to 150°. Fig 25.c shows that for d_2/d_1=2.0, Q/Q_o decreases with the increase of upstream and downstream cutoff wall depths.

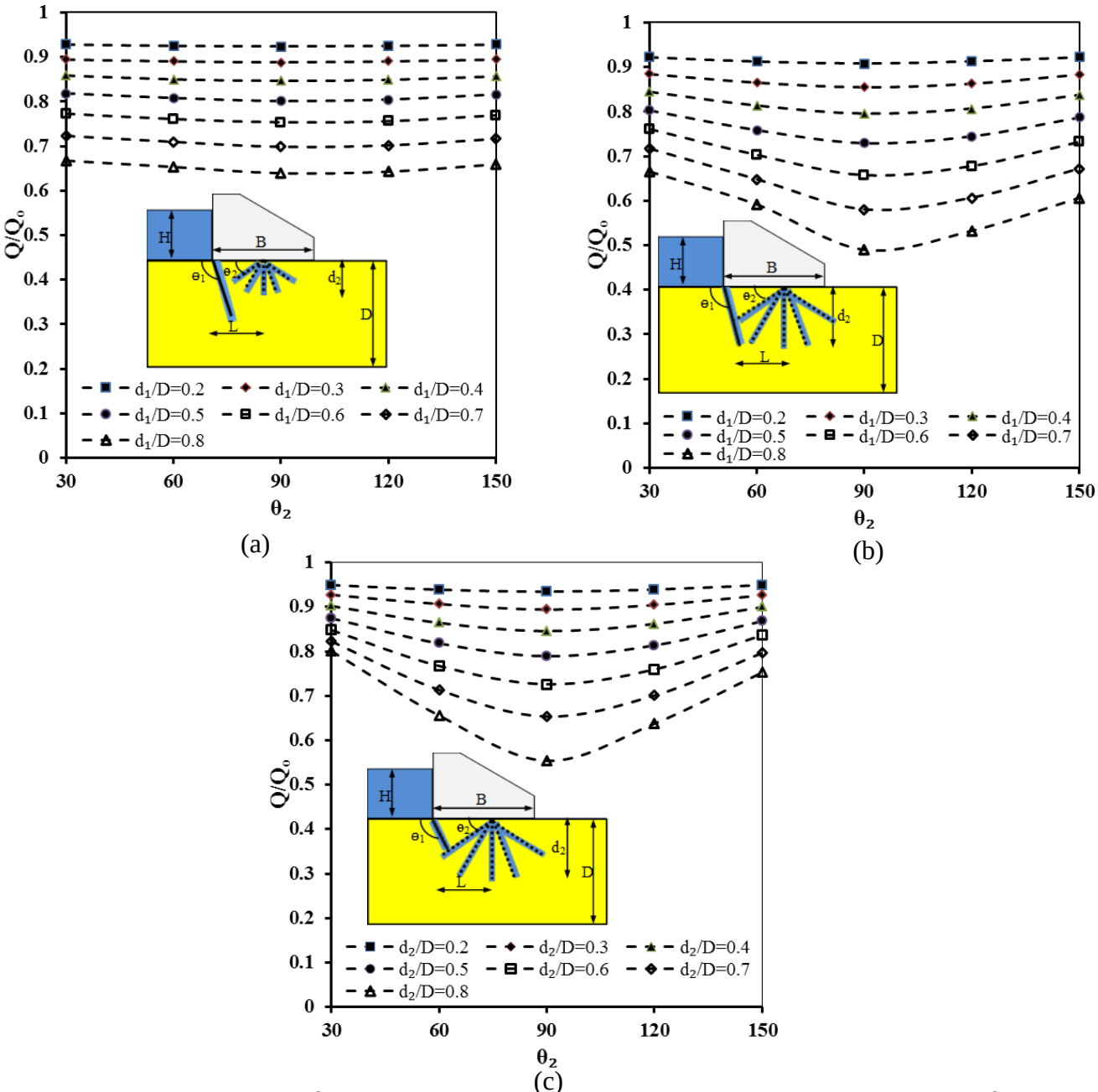

Fig. 25: Variation of relative seepage discharge (Q/Q_o) with the inclination angle of the downstream cutoff wall (θ_2) for θ_1=150°, L/B=0.5 and for d_2/d_1=0.5 (a), 1.0 (b), and 2.0 (c).

Figure 26 shows the same results as Figure 25 but for L/B=1.0. Fig 26a shows that for d_2/d_1=0.5, Q/Q_o decreases with the increase of θ_2. In addition, with the increases of cutoff wall depths, the value of Q/Q_o decreases slightly. Fig 26.b shows that for d_2/d_1=1.0, increasing the depths of the cutoff walls results in a decrease of Q/Q_o values. With d_2/d_1=1.0 (Fig 24.b), the resultant relative discharge Q/Q_o is relatively lower than the cases of d_2/d_1=0.5 and d_2/d_1=2.0 (Fig. 24.a and 24.c respectively). Installing the cutoff wall at the downstream end point with (L/B=1.0) results in a reduction and control of relative discharge Q/Q_o.

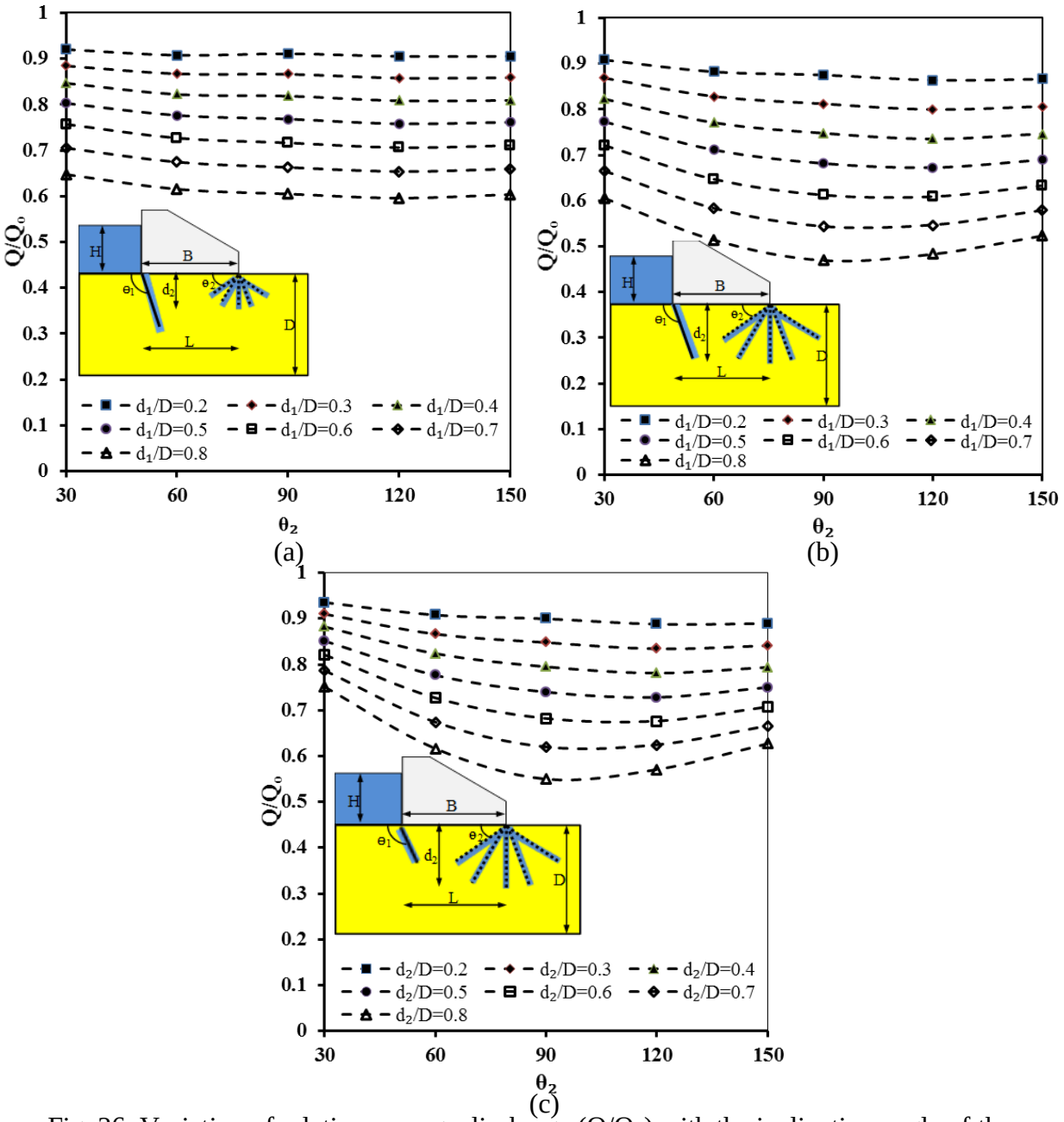

Fig. 26: Variation of relative seepage discharge (Q/Q_o) with the inclination angle of the downstream cutoff wall (θ_2) for θ_1=150°, L/B=1.0 and for d_2/d_1=0.5 (a), 1.0 (b), and 2.0 (c).

Summary on the effectiveness of inclined double cutoff walls in controlling the uplift force:

With the cutoff walls installed at the upstream and downstream ends (L/B = 1.0), when the depth of the downstream cutoff wall is greater than the depth of the upstream wall ($d_1 < d_2$), as the depths of the cutoff walls increase, the uplift force (U) increases and it exceeds the uplift force without the use of cutoff walls (U_o). Regarding the inclination angle of the downstream wall, increasing the value of θ_2 from 30° to 90°, leads to increase in the value of U and reaches the maximum value with θ_2 =90°, whereas it reduces again with θ_2 from 90° to 150°. In the case of $d_1 < d_2$ and L/B=0.5, as the depths of cutoff walls increase, the resultant uplift force decreases. The resultant value of U is less than U_o when the downstream cutoff wall is installed closer to the upstream wall (L/B = 0.5). In addition, with $d_1 < d_2$ and L/B=0.5, the inclination angle θ_1 =90° results in a slight increase in the uplift force U compared with θ_1= 60° and 150°. In these cases, ($d_1 < d_2$, L/B=0.5, and θ_1=60°, 90°, 120°), increasing the values of θ_2 leads to decrease in the value of U.

In the case of double cutoff walls with equal depth ($d_1 = d_2$), with L/B = 0.5, the uplift force decreases with increasing the cutoff wall depth and with decreasing θ_1 from 150° to 60°. For θ_1 = 60°, 90°, and 150°, the value of U shows little decrease with increasing θ_2. For $d_1 > d_2$ and L/B = 0.5, as the depth of the cutoff walls increases, the uplift force decreases. With respect to the inclination angle, for the same conditions, U shows a slight decrease for θ_1 = 90° compared to θ_1 = 60° and 120°. Moreover, increasing the inclination angle of the downstream cutoff wall results in a slight decrease in the resultant uplift force U for θ_1 = 60, 90°, and 150°. For $d_1 > d_2$ and L/B = 1.0, the uplift force decreases with increasing the depths of the cutoff walls. Regarding to the inclination angle θ_1, U shows the same behavior as in the previous case (L/B = 0.5) except for an increase in the inclination angle of the downstream cutoff wall resulting in a slight increase in U for θ_1 = 60, 90°, and 150°.

Fig. 27 shows the variation of relative uplift force (U/U_o) with the inclination angle of the downstream cutoff wall (θ_2). Figs. 27 a, b, c, d, e and f show the results for cutoff wall depth ratios of d_1/D=0.2, d_1 or d_2/D=0.2, d_2/D=0.2 ~~respectively, while Figs. 27 c, d, and e show that for cutoff wall depths~~ d_1/D=0.5, d_1 or d_2/D=0.5, and d_2/D=0.5 respectively. It can be concluded from the figures that installing the downstream cutoff wall closer to the upstream wall (L/B=0.5) results in more reduction of the relative uplift force U/U_o compared with installing the cutoff walls in the upstream and downstream end boundaries (L/B=1.0). With regards to the cutoff wall depths ratio d_2/d_1, increasing the depth of the upstream cutoff wall d_2/d_1=0.5 decreases the relative uplift force U/U_o more, followed by d_2/d_1=1.0 and d_2/d_1=2.0 respectively. In terms of the inclination angle of the upstream cutoff wall θ_1, installing the upstream cutoff wall with θ_1=60° results in more reduction in U/U_o, followed by θ_1=90° and 120° respectively. With regards to the inclination angle of the downstream cutoff walls θ_2, the resultant relative uplift force U/U_o decreases with increasing the value of θ_2 with L/B=0.5. On the other hand, U/U_o increases with increasing the value of θ_2 with L/B=1.0. Comparison of the results in Figs. 27 a, b, c with Figs. 27 c, d, e reveals that increasing the relative ratios of cutoff walls depths decreases the resultant uplift forces.

Among all the studied cases, installing the cutoff walls with $d_1 > d_2$, and the downstream cutoff wall closer to the upstream cutoff wall (L/B = 0.5), with the upstream cutoff wall inclined at θ_1=60°~~, and for different inclination angles of the downstream wall~~ shows the minimum resultant uplift force.

Summary on the effectiveness of inclined double cutoff walls in controlling the exit hydraulic gradient:

The results show that installing the cutoff walls in the upstream and downstream ends with L/B=1.0, can control and minimize the exit hydraulic gradient better, compared with the cutoff walls installed closer with L/B=0.50. With L/B=1.0 and different relative depths d_2/d_1=0.5, 1.0, 2.0, increasing the depths of the upstream and downstream cutoff walls decreases the resultant exit hydraulic gradient. For L/B=1.0, and different relative depths d_2/d_1=0.5, 1.0, 2.0, for all cases of inclination angle of the upstream cutoff wall θ_1=60°, 90°, 150°, increasing the inclination angle of the downstream cutoff wall from 30° to 150° results in a rapid reduction of the resultant exit gradient. But installing the upstream cutoff wall at right anle, θ_1=90°, causes reduction in the uplift force more than the cases of θ_1=60° and θ_1=150°. On the other hands, with L/B=1.0, for all cases of θ_1=60°, 90°, 150°, and for all cases of θ_2=30°, 60°, 90°, 120°, and 150°, installing the upstream and downstream cut off walls with equals depths d_1=d_2, results in the highest reduction of exit hydraulic gradient, followed by d_1>d_2, and by d_1< d_2.

In addition, with L/B=0.5, increasing the depths of upstream and downstream cutoff wall d_1 and d_2 causes the exit hydraulic gradient to decrease. With L/B=0.5, for all cases of inclination angle θ_1=60°, 90°, and 150°, and for different values of θ_2= 30°, 60°, 60°, 90°, 120°, and 150°, the case of equal depth of cutoff walls d_1=d_2 results in the highest reduction in the exit hydraulic gradient followed by $d_1 < d_2$ and $d_1 > d_2$. On the other hand, with L/B=0.5, for all cases of inclination angle θ_1=60°, 90°, and 150°, for different relative depths of d_2/d_1=0.5, 1.0, and 2.0, increasing the inclination angle of the downstream cutoff wall from θ_1=30° to 90° slightly decreases the value of exit hydraulic gradient whereas increasing the value of θ_1= from 90° to 150° results in a very little increase in the exit hydraulic gradient.

Fig. 28 presents the variation of relative exit hydraulic gradient (i/i_o) with the inclination angle of the downstream cutoff wall (θ_2) for six different relative depths of cutoff walls. Figs. 28 a, b, c, d, e, and f show the results for cutoff wall depth ratios d_1/D=0.2, d_1 or d_2/D=0.2, d_2/D=0.2, d_1/D=0.5, d_1 or d_2/D=0.5, and d_2/D=0.5 respectively. It can be concluded from the results that, installing the cutoff walls in the upstream and downstream end boundaries (L/B=1.0) reduces the resultant relative exit gradient more than the case of the downstream cut off wall installed closer to the upstream cutoff wall (L/B=0.5). The results also confirm that the inclination angle of downstream cutoff wall has a significant effect on the resultant exit gradient; the values of i/i_o decrease rapidly with the increase of θ_2 from 30° to 150°, especially for the case of L/B=1.0. The variation of inclination angle of upstream cutoff wall θ_1 has a small effect on the value of i/i_o. Installing the cutoff walls with equal depths d_2/d_1=1.0 results in more reduction in the exit hydraulic gradient, followed by d_2/d_1=0.5, and d_2/d_1=2.0 respectively.

For all the cases studied, installing the cutoff walls with equal depths (d_1=d_2), located in the upstream and downstream ends (L/B=1.0), and with angle of inclination for the upstream cutoff wall θ_1=60°, and inclination angle θ_2 ranging from 90° to 150° show the minimum resultant exit hydraulic gradient .

Summary on the effectiveness of inclined double cutoff walls to control seepage discharge:

The results show that installing the cutoff walls in the upstream and downstream ends of a hydraulic structure (L/B=1.0) reduces the seepage discharge rate more compared with L/B=0.50. With L/B=0.50, increasing the cutoff wall depth decreases the seepage discharge. With L/B=1.0, in case of equal depths of the two cutoff walls, d_1=d_2, among the different values of inclination angle of upstream cutoff wall, θ_1= 90° shows the minimum seepage discharge followed by the cases of d_1< d_2, and d_1> d_2 respectively. Installing the upstream cutoff wall at right angle, with L/B=0.5 or L/B=1.0, for different relative depths d_2/d_1=0.5, 1.0, and 2.0 introduces the least values of seepage discharge followed by θ_1=60°, and θ_1=150° respectively. With L/B=0.5 or L/B=1.0, and d_2/d_1=0.5, for different values of θ_1, the resultant seepage discharge increases

slightly with increasing θ_2 from 30° to 150°. On the other hand, with L/B=0.5 or L/B=1.0, and d_2/d_1=1.0 and 2.0, for different values of θ_1, the resultant seepage discharge decreases slightly with increasing the inclination angle of the downstream cutoff wall from 30° to 90° and shows a very little increase when the value of θ_2 increases from 90° to 150°.

Fig. 29 shows the variation of relative seepage discharge (Q/Q_o) with the inclination angle of the downstream cutoff wall (θ_2) for six different cases of relative cutoff wall depths. Figs. 29 a, b, c show the results for shallow cutoff wall depth ratios d_1/D=0.2, d_1 or d_2/D=0.2, and d_2/D=0.2 respectively, and Figs. 29 c, d, and e show the results for deep cutoff wall depth ratios d_1/D=0.5, d_1 or d_2/D=0.5, and d_2/D=0.5 respectively. Installing the cutoff walls in the upstream and downstream end boundaries (L/B=1.0) results in a greater reduction of the seepage discharge compared with (L/B=0.5). The resultant seepage discharge Q/Q_o is minimum in case of inclination angle of the upstream cutoff wall θ_1 = 60° followed by 90° and 120° respectively. Installing the upstream and downstream cutoff walls with equal depths d_2/d_1=1.0 results in more decrease in the resultant seepage discharge followed by d_2/d_1=0.5, and d_2/d_1=2.0 respectively. Increasing the cutoff wall depth ratios has a significant effect on reducing the resultant seepage discharge. For the shallow cutoff depths, the inclination angle of the downstream cutoff wall has less impact of the resultant Q/Q_o, while with deeper depths, the right angle of downstream cutoff wall θ_2=90° results in more reduction in Q/Q_o.

For all studied cases, installing the cutoff walls with equal depths (d_1=d_2) located in the upstream and downstream ends (L/B=1.0), and angle of inclination for the upstream cutoff wall θ_1=60°, with right angle for the downstream cutoff walls $\theta_{2=}$ 90° presents the minimum value of resultant seepage discharge compared with the other studied cases.

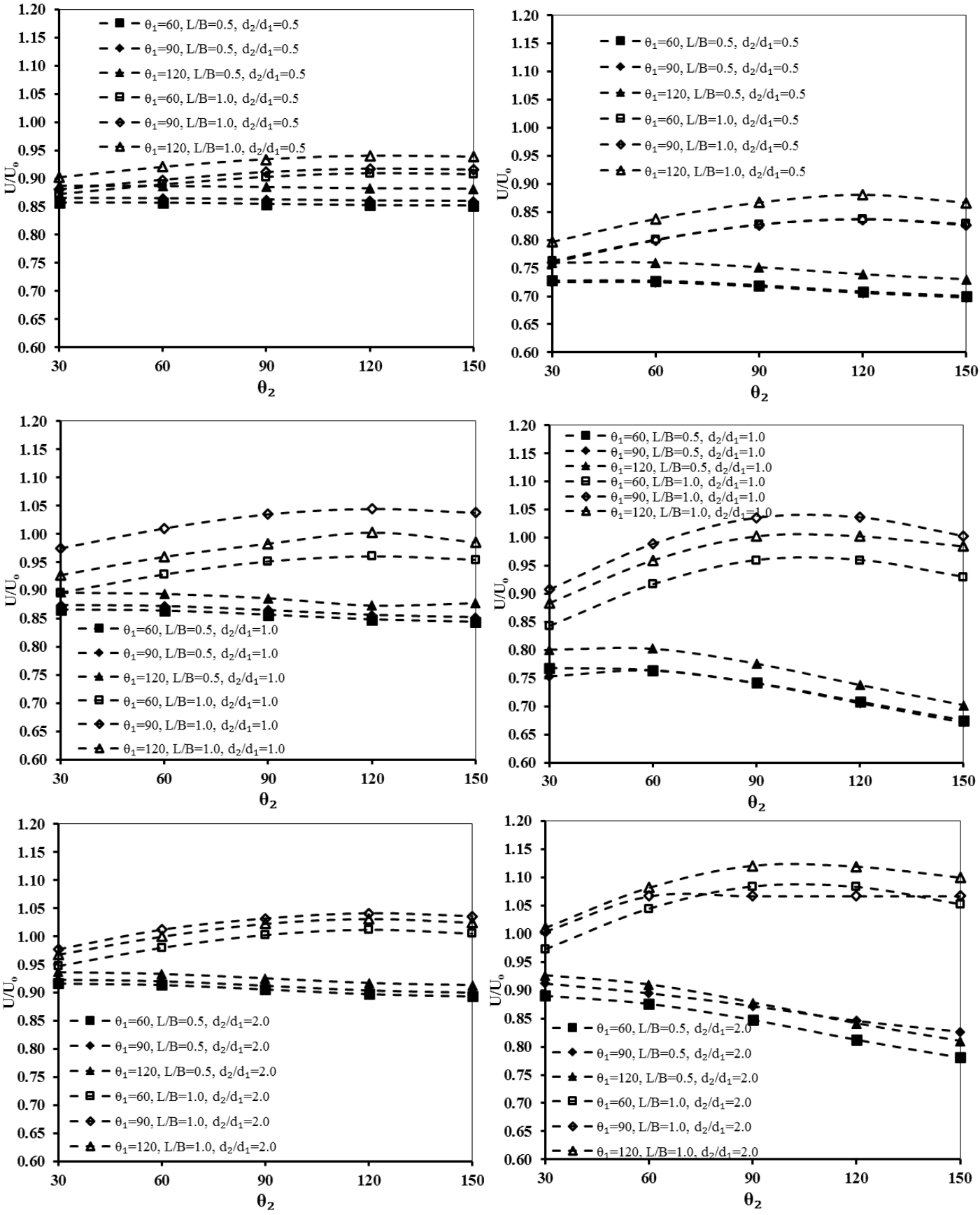

Fig. 27: Variation of relative uplift force (U/U_o) with the inclination angle of the downstream cutoff wall (θ_2) for defined values of θ_1, L/B, d_2/d_1, and for (a) d_1/D=0.2, (b) d_1 or d_2/D=0.2, (c) d_2/D=0.2, (d) d_1/D=0.5, (e) d_1 or d_2/D=0.5, (f) d_2/D=0.5

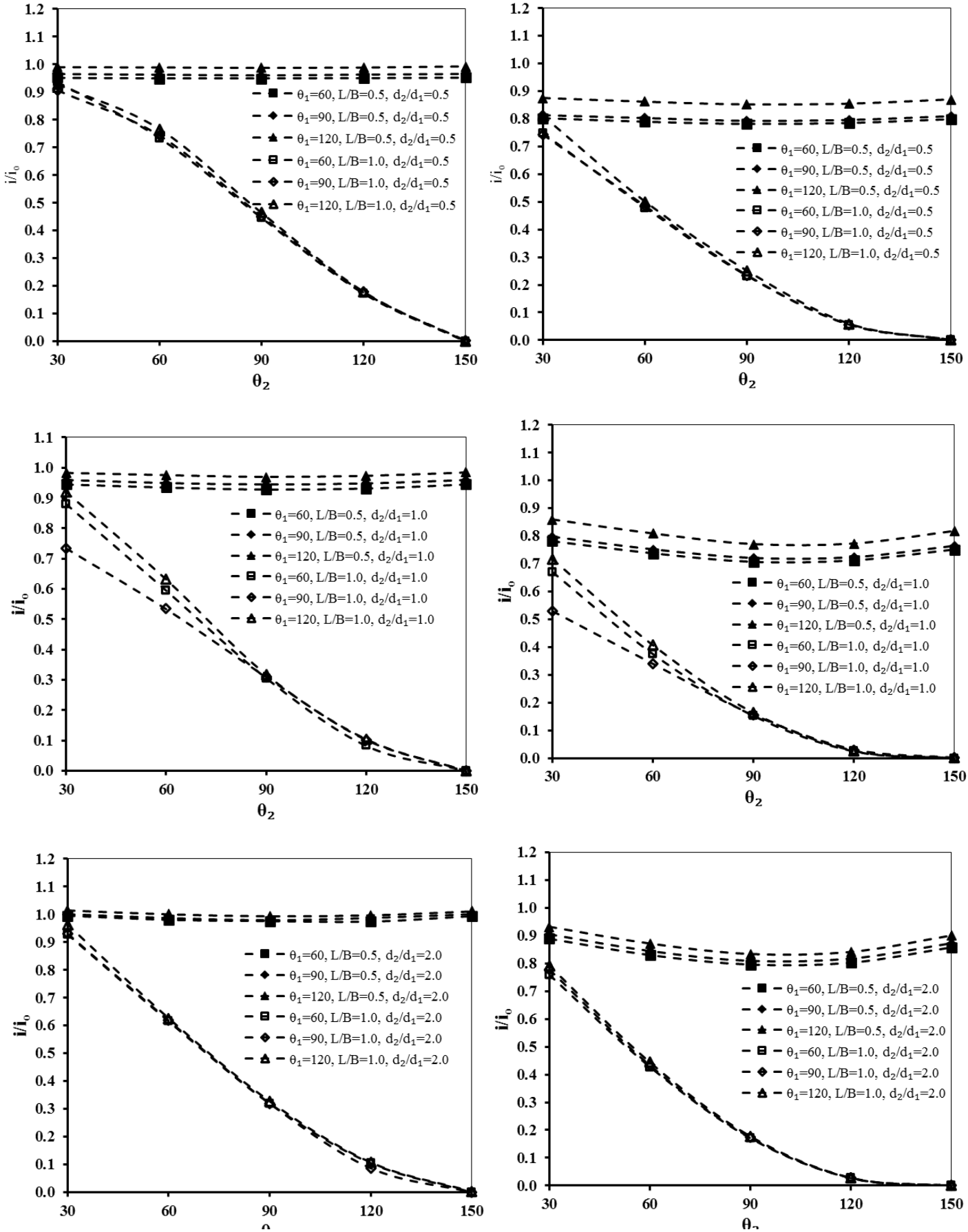

Fig. 28: Variation of relative exit hydraulic gradient (i/i_o) with the inclination angle of the downstream cutoff wall (θ_2) for defined values of θ_1, L/B, d_2/d_1, and for (a) d_1/D=0.2, (b) d_1 or d_2/D=0.2, (c) d_2/D=0.2, (d) d_1/D=0.5, (e) d_1 or d_2/D=0.5, (f) d_2/D=0.5

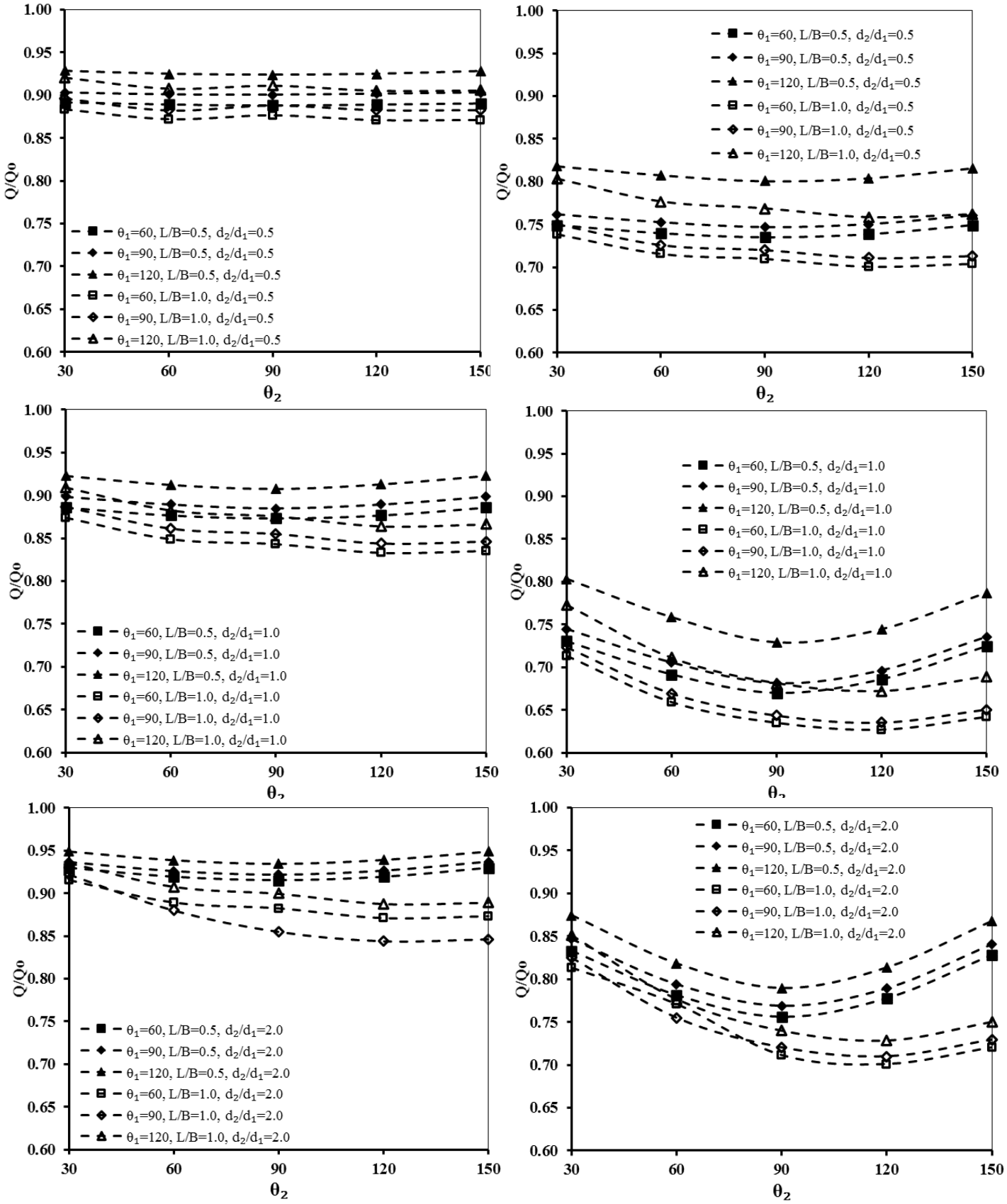

Fig. 29: Variation of relative seepage discharge (Q/Q_o) with the inclination angle of the downstream cutoff wall (θ_2) for defined values of θ_1, L/B, d_2/d_1, and for (a) d_1/D=0.2, (b) d_1 or d_2/D=0.2, (c) d_2/D=0.2, (d) d_1/D=0.5, (e) d_1 or d_2/D=0.5, (f) d_2/D=0.5

Conclusion

To the best of authors' knowledge, the effectiveness of using inclined double cutoff walls beneath hydraulic structures has not been studied before. Previous research studied single cutoff wall, inclined cutoff wall, and vertical double cutoff walls. A recent study investigated the effect of using vertical double cutoff walls with different depths and locations. The current research has studied the effectiveness of using inclined cutoff walls beneath hydraulic structures. The effect of different configurations of inclined double cutoff walls on the uplift force, exit hydraulic gradient, and seepage discharge were investigated. The studied variable parameters were upstream cutoff wall depth d_1, downstream cutoff wall depth d_2, distance between cutoff walls L, inclination angle of the upstream cutoff wall (θ_1), and inclination angle of the downstream cutoff wall (θ_2). The Finite Element Method (FEM) was used to solve the governing equations of groundwater flow with assigned boundary conditions. For model validation, the numerical results were compared with the analytical solution for the case of vertical double cutoff walls with equal depth, located in the upstream and downstream ends of a hydraulic structure. The resulted error between the numerical and analytical solutions was 5.0%. After model validation, several cases were simulated numerically to study the effects of the following parameters d_1, d_2, θ_1, θ_2, U, i, and Q. The main findings of the current study are summarized as follows:

For the uplift pressure, installing the upstream cutoff wall with greater depth than the downstream wall ($d_1 > d_2$) reduces the value of uplift force, U. On the other hand, installing the downstream cutoff wall deeper than the upstream wall ($d_2 > d_1$) affects negatively on the resultant uplift force (increases the values of U). Installation of the downstream cutoff wall closer to the upstream wall (L/B=0.5) reduces the value of U compared with the case of L/B=1.0. The case of L/B=0.5, $d_1 > d_2$, and the upstream cutoff wall with angle of θ_1=60^o, shows minimum resultant uplift force compared with θ_1=90^o and 150^o and the values of U decrease slightly with the increase of θ_2 from 30^o to 150^o.

Installing the upstream cutoff wall with greater depth than the downstream wall ($d_1 > d_2$) affects negatively on the exit hydraulic gradient (increases the values of i). On the other hand, installing the downstream cutoff wall deeper than the upstream wall ($d_2 > d_1$) affects positively on the exit hydraulic gradient (reduces the values of i). Installation of the cutoff walls in the upstream and downstream ends (L/B=1.0) reduces the exit hydraulic gradient more compared with the case of L/B=0.50. The case of L/B=1.0, equal depths of cutoff walls $d_2 = d_1$, and the upstream cutoff wall installed with angle θ_1=60^o, shows minimum value of exit hydraulic gradient compared with θ_1=90^o and 150^o and the values of i decease rapidly with increasing θ_2 from 30^o to 150^o. The inclination angle of the downstream cutoff wall (θ_2) has a significant effect on the control and reduction of the exit hydraulic gradient, especially in case of L/B=1.0, for different values of θ_1.

Deeper upstream and downstream cutoff walls affect positively on the seepage discharge (reduce the values of Q). Installation of cutoff walls in the upstream and downstream ends of hydraulic structures (L/B=1.0) reduces the resultant seepage discharge more compared with the case of L/B=0.50. With L/B=1.0, equal depths of upstream and downstream cutoff walls (d_1=d_2) result in more reduction in seepage discharge compared with $d_2 > d_1$ and $d_1 > d_2$. The case of L/B=1.0, d_1=d_2, and the upstream and downstream cutoff walls installed with angles θ_1=60^o and θ_2=90^o respectively, shows minimum resultant seepage discharge compared with other cases of inclined upstream and downstream cutoff walls.

References

Ahmed AA, Bazaraa AS. Three-dimensional analysis of seepage below and around hydraulic structures, Journal of Hydrologic Engineering, ASCE, 2009, No. 3, Vol. 14, pp. 243-247.

Ahmed AA. Design of hydraulic structures considering different sheet pile configurations and flow through canal banks, Computers and Geotechnics, 2011, No. 4, Vol. 38, pp. 559-565.

Abedi Koupaei J. Investigation of effective elements on uplift pressure upon diversion dams by using finite difference, thesis for MSC (in Persian), University of Tarbiat Modarres, Tehran, Iran, 1991.

Bligh, W.G., 1910. Dams, barrages and weirs on porous foundations. Eng. News 64 (26), 708–710.

Chawla, A.S., Kumar, A., 1983. Stability of structure with two end cutoffs. J. Inst. Eng. Civil Eng. Division (India) 63 (5), 272–279.

Fil'chakov PF. The theory of filtration beneath hydrotechnical structures, Vol. 2, Izd-vo Akademii nauk Ukrainskoi SSR, Kiev, 1960.

Geo-Studio, User manual, Geo-Studio-2012 2012 GEOSLOPE International Calgary.

Griffiths DV, Fenton GA. Three-dimensional seepage through spatially random soil, Journal of Geotechnical and Geoenviromental Engineering, 1997, Vol. 123, pp. 153- 160.

Goel, A., Pillai, N.N., 2010. Variation of exit gradient downstream of weirs on permeable foundations. Pacific J. Sci. Tech. 11 (1), 28–36.

Harr ME. Groundwater and Seepage, McGraw-Hill, New York, 1962.

Jafarieh A, Ghannad M. The Effect of Foundation uplift on Elastic Response of Soil-Structure Systems, International Journal of Civil Engineering, 2014, No. 2, Vol. 12, pp. 146-157.

Jain, A., Reddi, M., 2011. Finite-Depth Seepage below Flat Apron with Equal End Cutoffs. J. Hydraulic. Eng. (137), (12):1659-1667. https://doi.org/10.1061/(ASCE)HY.1943-7900.0000459.

Krahn J. Seepage modeling with Seep/w, An Engineering Methodology, Calagary, Alberta, Canada, 2007.

Khosla, A.N., Bose, N.R., Taylor, E.M. 1936. Design of weirs on permeable foundations. Publication No. 12, Central Board of Irrigation, New Delhi, India.

Lane, E.W., 1935. Security from under-seepage masonry dam on earth foundations. Trans. Am.Soc. Civ. Eng. 60 (4), 929–966.

Malhotra, J.K. 1936. Appendix to Chapter VII: Mathematical investigations of the subsoil flow under two standard forms of structures. Publication No. 12, Central Board of Irrigation, New Delhi, India, 85–90.

Najjar, Y., Naouss, W. 1999. Finite element-based seepage design charts for sheet piles penetrating heterogeneous media. Transportation Research Record 1663, Transportation Research Board, Washington, DC, 64–70.

Nourani, B., Salmasi, F., Abbaspour, A., Oghati Bakhshayesh, B., 2017. Numerical investigation of the optimum location for vertical drains in gravity dams. Geotech. Geol. Eng. 35 (2), 799–808. https://doi.org/10.1007/s10706-016-0144-1.

Opyrchal L. Application of fuzzy sets to identify seepage path through dams, Journal of Hydraulic Engineering, ASCE, 2003, No. 7, Vol. 129, pp. 546-548.

Pavlovsky NN. The theory of ground water flow beneath hydrotechnical structures, Research Melioration Institute, Petrograd, USSR, 1922 (in Russian).

Pavlovsky NN. Collected works, Izd. AN SSSR Moscow - Leningrad, USSR, 1956.

Polubarinova-Kochina PY. Theory of groundwater movement, Trans. JM. Roger de Wiest, Princeton University, Princeton, NJ, 1962.

Rahmani Firoozjaee A, Afshar M. Discrete least square method (DLSM) for the solution of free surface seepage problem. International Journal of Civil Engineering, 2007, No. 2, Vol. 5, pp. 134-143.

Salmasi, F., Nouri, M., 2017. Effect of upstream semi-impervious blanket of embankment dams on seepage. ISH J. Hydraulic Eng. 25 (2), 143–152. https://doi.org/10.1080/09715010.2017.1381862.

Salmasi, F., Mansuri, B., Raoufi, A., 2015. Use of numerical simulation to measure the effect of relief wells for decreasing uplift in a homogeneous earth dam. Civil Eng. Infrastruct. J. 48 (1), 35–45. https://doi.org/10.7508/CEIJ.2015.01.004.

Sedghi-Asl M, Rahimi H, Khaleghi H. Effect of cutoff wall's depth and situation on reducing seepage under hydraulic structures by using numerical method, 5th Iranian Hydraulic Conference, Iran, 2005 (In persian).

Sedghi-Asl M, Rahimi H, Khaleghi M. Laboratory investigation of the seepage control measures under coastal dikes, Experimental Techniques, 2011, No. 1, Vol. 36, pp. 61-71.

Zainal EAK. The effects of cutoff wall angle on seepage under dams, Journal of Engineering, 2011, No. 5, Vol. 17, pp. 1109-1131.

Zienkiewicz OC. The Finite Element Method, McGraw- Hill, New York, 1977.